energies

MDPI

Article

Study of the EU-DEMO WCLL Breeding Blanket Primary Cooling Circuits Thermal-Hydraulic Performances during Transients Belonging to LOFA Category

Cristiano Ciurluini [1,*], Fabio Giannetti [1], Alessandro Del Nevo [2] and Gianfranco Caruso [1]

[1] Dipartimento di Ingegneria Astronautica, Elettrica ed Energetica, Sapienza University of Rome, 00186 Rome, Italy; fabio.giannetti@uniroma1.it (F.G.); gianfranco.caruso@uniroma1.it (G.C.)
[2] ENEA FSN-ING-SIS, ENEA CR Brasimone, Località Brasimone, 40032 Camugnano, Italy; alessandro.delnevo@enea.it
* Correspondence: cristiano.ciurluini@uniroma1.it

Abstract: The Breeding Blanket (BB) is one of the key components of the European Demonstration (EU-DEMO) fusion reactor. Its main subsystems, the Breeder Zone (BZ) and the First Wall (FW), are cooled by two independent cooling circuits, called Primary Heat Transfer Systems (PHTS). Evaluating the BB PHTS performances in anticipated transient and accident conditions is a relevant issue for the design of these cooling systems. Within the framework of the EUROfusion Work Package Breeding Blanket, it was performed a thermal-hydraulic analysis of the PHTS during transient conditions belonging to the category of "Decrease in Coolant System Flow Rate", by using Reactor Excursion Leak Analysis Program (RELAP5) Mod3.3. The BB, the PHTS circuits, the BZ Once Through Steam Generators and the FW Heat Exchangers were included in the study. Selected transients consist in partial and complete Loss of Flow Accident (LOFA) involving either the BZ or the FW PHTS Main Coolant Pumps (MCPs). The influence of the loss of off-site power, combined with the accident occurrence, was also investigated. The transient analysis was performed with the aim of design improvement. The current practice of a standard Pressurized Water Reactor (PWR) was adopted to propose and study actuation logics related to each accidental scenario. The appropriateness of the current PHTS design was demonstrated by simulation outcomes.

Keywords: DEMO; primary heat transfer system; balance of plant; RELAP5; loss of flow accident; once through steam generators

Citation: Ciurluini, C.; Giannetti, F.; Del Nevo, A.; Caruso, G. Study of the EU-DEMO WCLL Breeding Blanket Primary Cooling Circuits Thermal-Hydraulic Performances during Transients Belonging to LOFA Category. *Energies* **2021**, *14*, 1541. https://doi.org/10.3390/en14061541

Academic Editor: Guglielmo Lomonaco

Received: 5 February 2021
Accepted: 8 March 2021
Published: 11 March 2021

1. Introduction

In the European DEMO (EU-DEMO) fusion reactor, the Breeding Blanket (BB) component accomplishes several functions [1,2]. Firstly, it acts as a cooling device. The nuclear interactions between the neutrons produced within the plasma and the lithium contained in the breeder allow to convert the neutron kinetic energy in thermal power to be removed. The same nuclear reactions are supposed to be used to produce the tritium fuel needed to reach the self-sufficiency. Moreover, the breeding blanket serves as shielding, preventing the high-energy neutrons from escaping outside the reactor and protecting from damage the more radiation-susceptible components, like the superconducting magnets.

In the framework of the EUROfusion Programme, two breeding blanket concepts were selected for the EU-DEMO R&D strategy: Water-Cooled Lithium-Lead (WCLL) and Helium-Cooled Pebble Bed (HCPB) [1]. These two technologies will also be tested in the ITER fusion reactor, according to the goals of the ITER Test Blanket Module (TBM) programme [1]. The main outcome of this experimental campaign will be the Return of Experience for the EU-DEMO Breeding Blanket Programme [3]. The computational activity presented in this paper deals with the WCLL option. It foresees the usage of water at typical Pressurized Water Reactor (PWR) thermodynamic conditions (295–328 °C and 15.5 MPa)

as coolant [1,2]. The blanket relies on liquid lithium-lead as breeder, neutron multiplier and tritium carrier and on Eurofer as structural material. An armour, consisting of a thin tungsten layer is assumed to cover the First Wall (FW) component (plasma-facing surface).

The cooling systems associated to the principal blanket subsystems, namely the FW and the Breeder Zone (BZ), are called Primary Heat Transfer Systems (PHTS) [2,4]. Their main function is to provide primary coolant at the required thermodynamic conditions. The thermal power they remove is then delivered to the Power Conversion System (PCS) to be converted into electricity [5,6].

With the aim of the design improvement, the evaluation of the BB PHTS thermal-hydraulic (TH) behavior during anticipated transient and accident conditions is a key issue. To achieve this goal, computational activities can be performed by using best estimate system codes. Principally, system codes adopt a one-dimensional approach to solve the balance equations. For this reason, they are more recommended for simulations involving circuits, where the fluid main stream direction can be clearly identified. They allow to simulate the overall primary cooling system, including the pipelines and all the vessel components (pumps, heat exchangers, pressurizer). However, in some of them, also 3D approaches are partially implemented, such as in RELAP5-3D [7], CATHARE-3 [8], SAM [9], and so they can also be used for components characterized by more complex fluid flow paths. Throughout decades, these codes have been validated for Light Water Reactors (LWR), simulating a wide range of transient and accidental scenarios. Hence, their usage can also be envisaged for WCLL blanket, whose primary coolant has similar thermodynamic conditions.

In the last years, a large experience was matured in the simulation of transients involving fusion reactors. Referring to EU-DEMO WCLL PHTS, both the in-vessel [10] and ex-vessel [11] Loss Of Coolant Accidents (LOCA) were investigated with MELCOR code, [12]. The main simulation purpose was assessing the hydrogen production and the radiological source term mobilization in order to demonstrate the consistency of the EU-DEMO design with the safety and environmental criteria. MELCOR code was also used for a parametrical study in support of the reactor Vacuum Vessel Pressure Suppression System design, as described in [13]. A preliminary analysis of the Loss Of Flow Accident (LOFA) is reported in [14]. In this case, RELAP5/Mod3.3 code [15] was used to perform a TH-oriented transient calculation aimed at the sizing of the flywheel to be adopted for the PHTS Main Coolant Pumps (MCPs).

For what concerns the EU-DEMO HCPB PHTS, RELAP5-3D code was properly integrated with a computational fluid-dynamic code in order to investigate the thermal-hydraulic performances of the primary circuits during an Ex-Vessel LOCA scenario, [16]. With the same code, multiple LOFA scenarios were also studied [17]. LOCA transients were also simulated with MELCOR code [18]. The activity goal was to perform a parametric study on the break size and to assess its impact on some reactor relevant parameters, such as containment pressure and FW component maximum temperature.

System codes were largely adopted also in the framework of research activities related to China Fusion Engineering Test Reactor (CFETR) and Korean DEMO (K-DEMO) Reactor. CFETR design foresees a Water-Cooled Ceramic Breeder (WCCB) blanket concept. RELAP5/Mod3.3 code was employed for transient analysis involving LOFA, [19], and Loss of Heat Sink (LOHS), [20], scenarios. The calculations allowed an in-depth evaluation of the WCCB blanket behavior. As initial conditions, different fusion power modes were considered.

One of the blanket concepts proposed for K-DEMO reactor is the water-cooled multiple-layer breeding blanket. It consists of a sandwich of multiple layers of breeder (Li_4SiO_4) and multiplier ($Be_{12}Ti$) mixtures, cooling channels, and structural materials. They are stacked in the radial direction, parallel to the first wall. MELCOR was adopted to investigate the reactor response after a vacuum vessel rupture, mainly focusing on hydrogen production and dust explosions, [21].

System codes also allow to study operational transients and to conceptually design the machine control system. This is a relevant design issue for fusion reactors where a plasma pulsed operating regime is foreseen (including both pulse and dwell phases). Similar studies were conducted for all the aforementioned fusion reactor concepts: EU-DEMO HCPB, [14], with RELAP5-3D; EU-DEMO WCLL, [16], with RELAP5/Mod3.3; CFETR, [22], with RELAP5/Mod3.3; K-DEMO, [23], with Multi-dimensional Analysis of Reactor Safety (MARS-KS) [24].

The calculations presented in this paper were performed within the framework of the EUROfusion Work Package Breeding Blanket, by using a modified version of RELAP5/Mod3.3 code, [25]. This new extended version was developed at the Department of Astronautical, Electrical and Energy Engineering (DIAEE) of Sapienza University of Rome, in order to enhance the code capability in simulating fusion reactors. New features implemented include new working fluids (lithium-lead, HITEC® molten salt), new heat transfer correlations, etc. The selected transients to be investigated belong to the category of "Decrease in Coolant System Flow Rate". The considered Postulated Initiating Events (PIE) consist in both the partial and complete LOFA occurring either in BZ or in FW PHTS. In addition, the influence of the loss of off-site power, occurring in combination with PIE, was studied.

In the following, Section 2 offers a brief description of EU-DEMO WCLL reactor configuration. In Section 3, it is described the RELAP5/Mod3.3 model developed to simulate the blanket component and the related primary heat transfer systems. Calculation results are collected in Section 4. Full plasma power state is commented in Section 4.1, while transient simulations are fully analyzed in Section 4.2. A final discussion on the main outcomes of the computational activity is reported in Section 5. The conclusive remarks related to the current work are contained in Section 6. Moreover, at the end of the paper, it is provided a list of the main acronyms used in the text.

2. Short Overview of EU-DEMO WCLL Reactor Configuration

DEMO reactor normal operations are characterized by a pulsed operating regime. It consists in eleven pulses per day, each one made up of a full-power burn time (pulse) of two hours and a dwell time of 10 min [6]. The reference parameters and baseline are those of DEMO 2017 concept [2]. The reactor Computer Aided Design (CAD) model is shown in Figure 1 [2,4,5], including all the PHTS components located inside and outside the Vacuum Vessel.

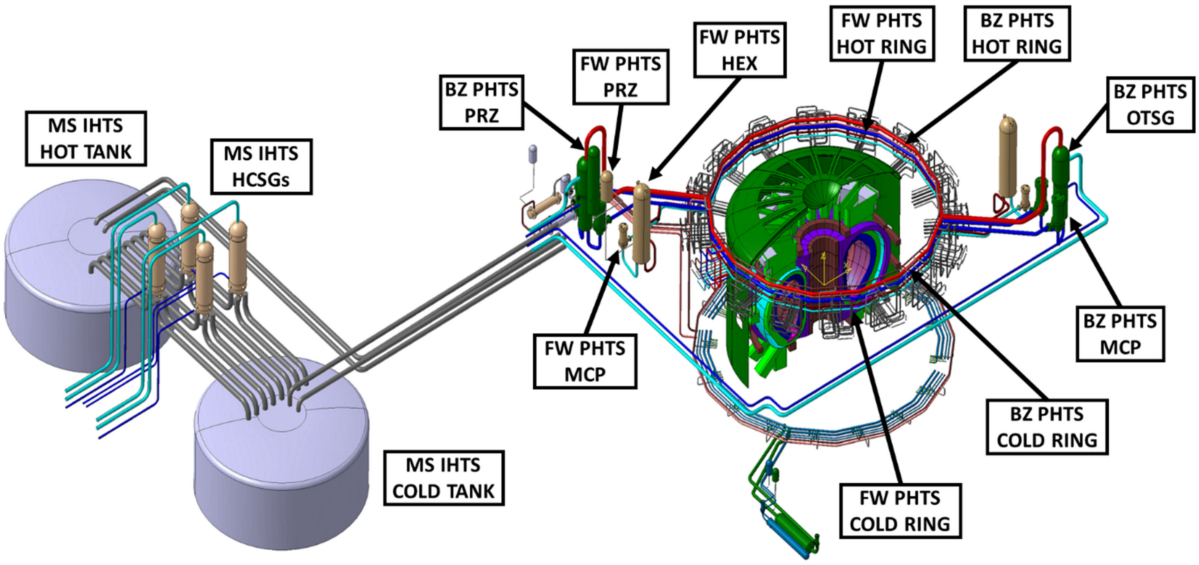

Figure 1. Reactor CAD model, DEMO 2017 baseline [2,4,5]. Overview of the tokamak, the primary cooling systems and the molten salt intermediate circuit and storage tanks.

The reference design adopted for DEMO blanket is the WCLL2018.v0.6, based on Single Module Segment (SMS) approach [2,4]. The overall component is constituted by 16 identical sectors, each one occupying 22.5° in the toroidal direction. Each sector is furtherly divided in In Board (IB) and Out Board (OB) blankets, located radially inwards and outwards with respect to the plasma chamber. At its time, OB is toroidally composed by 3 SMSs named Left OB (LOB), Central OB (COB) and Right OB (ROB), while IB is partitioned only in two SMSs, called Left IB (LIB) and Right IB (RIB). In conclusion, five segments are associated to each DEMO sector.

Each single segment is made up of about 100 breeding cells (BRC), distributed along the poloidal (vertical) direction. The BRC layout is differentiated between segments (especially between OB and IB segments) and, in the same segment, varies according to the poloidal position. The BRC design used as reference for modelling purposes is the one of the COB equatorial cell. Its detailed description can be found in [26,27]. In the BRC, the component facing the plasma chamber is called First Wall (FW). It is protected by a tungsten armor and cooled with water flowing in square channels equally distributed along the poloidal height. The liquid lead-lithium (LiPb) acts as breeder. It enters the BRC from the bottom, flows in the radial direction, from the BRC Back Plate (BP) to the FW, rises poloidally and then turns back radially, from the FW to the BP, exiting through an outlet pipe. The breeder zone refrigeration is assured by a batch of radial-toroidal C-shaped Double Walled Tubes (DWTs). They are displaced in horizontal planes at different poloidal elevations and are split into three arrays along the radial direction. In this way, their cooling capability is uniformly distributed in all the BZ volume. The back part of the breeding cell in the radial direction is devoted to house both LiPb and water manifolds. Finally, the back supporting structure is a continuous steel plate in poloidal direction representing the backbone of the blanket segment. The layout for COB equatorial cell is shown in Figure 2 [2,4].

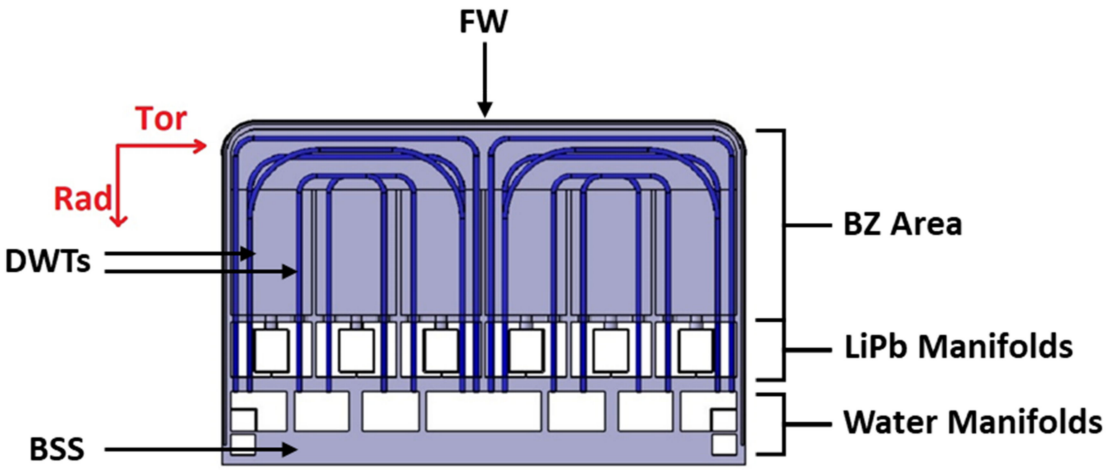

Figure 2. EU-DEMO Water Cooled Lithium-Lead (WCLL) blanket component: detail of the Central Outboard (COB) equatorial breeding cell, WCLL2018.v0.6 design [2,4].

The blanket component is provided with two independent cooling systems: the BZ PHTS and the FW PHTS. The former removes the nuclear heat generated in the breeder zone by the interactions between the lead-lithium and the neutrons coming from the plasma. The latter cools the FW component which is heated up by the incident Heat Flux and by the neutron wall load. The simulation activity presented in this paper is related to the indirect coupling option [4,6]. In this configuration, the BZ PHTS delivers thermal power directly to the PCS, by means of two Once-Through Steam Generators (OTSG). Instead, the FW PHTS, thanks to two water/molten salt Heat EXchangers (HEXs), is connected to an Intermediate Heat Transfer System (IHTS) provided with an Energy Storage System (ESS). The ESS function is to flatten the pulsed source term (plasma power), according to

the design requirement of continuous and nearly constant electrical power delivered to the grid. The ESS accumulates a fraction of the FW thermal power during the plasma pulse and delivers it to the PCS during the dwell time. The power fraction to be accumulated during pulse is calculated to obtain a constant turbine load during the overall operating regime (pulse and dwell). The energy storage is constituted by a system of two tanks filled with molten salt at different temperatures. During pulse, there is a net HITEC® flow rate going from the cold tank to the hot one and here accumulated. During dwell, the hot molten salt flows through four Helicoidal Coil Steam Generators (HCSGs) and power is delivered to the PCS. The current PHTS design foresees two loops for each system. They are symmetrically disposed along the tokamak circumference (i.e., toroidal direction). The main PHTS components (for both BZ and FW cooling circuits) are:

- The hot and cold rings, circular collectors (hot) and distributors (cold) of the overall PHTS mass flow from/to the loops and to/from each of the tokamak sectors, respectively.
- The sector manifolds, differentiated in collectors and distributors, respectively connecting the tokamak sectors to the hot ring and the cold ring to the tokamak sectors.
- The loop piping (hot legs, cold legs, loop seals), linking the main vessel components.
- The BZ OTSGs and the FW HEXs.
- The MCPs, providing the primary coolant flow.
- The pressurizer system, one per PHTS, ensuring the pressure control function.

The location of each component in the overall cooling systems is shown in Figure 1. For modelling purposes, the PCS and IHTS system sections considered are only the BZ OTSGs and FW HEXs secondary sides.

3. RELAP5 Thermal-Hydraulic Model

Referring to the reactor configuration outlined in the previous section, a full model of the DEMO WCLL BB PHTS was prepared to perform transient calculations. The main modelling approach considered while developing the input deck was the "slice nodalization" technique. This means that a common vertical mesh was used for all the system components at the same elevation. In addition, the node-to-node ratio, defined as the ratio between the length of two adjacent control volumes (CVs), was kept below 1.25 in the entire model. The respect of this upper limit represents an important criterion to avoid numerical errors due to an inhomogeneous mesh. For all the vessel components and piping, actual design elevations were strictly maintained to avoid inconsistencies mainly in the evaluation of the natural circulation. Fluid and material inventories were rigorously maintained for both BB and PHTS cooling systems.

3.1. Blanket Model

From the hydrodynamic point of view, the BZ and FW cooling circuits were independently simulated. Nevertheless, the two systems are thermally coupled inside the BRC. For this, RELAP5 heat structure components were used to simulate in detail the heat transfer phenomena taking place within the breeding cell. During transient simulations, the BZ and FW thermal coupling has a significant influence on the circuit TH behavior.

As already pointed out, each DEMO sector is constituted by five poloidal segments (three for OB and two for IB). The BZ and FW cooling circuits here contained were collapsed in some equivalent pipe components, three for each PHTS. The OB and IB segments were grouped as following: LOB/ROB, COB, LIB/RIB.

For both BZ and FW PHTS, the equivalent pipes model the overall water flow path inside the vacuum vessel. The components associated to each segment and considered for simulation purposes are: (1) inlet Feeding Pipe (FP); (2) inlet spinal water manifold; (3) DWTs or FW channels; (4) outlet spinal water manifold; (5) outlet FP. The CVs belonging to the equivalent pipes are characterized by different hydraulic properties (flow area, hydraulic diameter, etc.) in order to properly simulate all the aforementioned components. For the equivalent pipes corresponding to LOB/ROB and LIB/RIB, the CVs flow area

and hydraulic diameter, as well as the water mass flow, were evaluated considering the reference data belonging to both segments. In this way, the pressure drops through these components were correctly modelled. The PHTS sector collectors and distributors, mentioned in Section 2, are connected to the FPs thanks to inlet and outlet manifolds, closing the overall PHTS circuit. In conclusion, for each PHTS (either BZ or FW) and for each sector, five equivalent pipes and two branches were used. Pipe components correspond to: sector distributor (P1); water circuit inside LOB and ROB (P2); water circuit inside COB (P3); water circuit inside LIB and RIB (P4); sector collector (P5).

Regarding the BRC, the most studied design belongs to the cell located at the equatorial plane of COB [2,26,27]. For this reason, it was adopted as reference and also used for all the other BRCs poloidally distributed along the overall segment. Concerning the BRCs of ROB, LOB, LIB, RIB segments, the reference layout was scaled by using the material inventories derived from the CAD model [2,4,5].

About the DWTs, since these components are in parallel within the BRC, they were collapsed and modelled by using the central batch of CVs of P2, P3, P4 equivalent pipes, the ones related to BZ PHTS. As discussed in Section 2, they are split into three arrays along the radial direction. Moreover, their C-shape in the radial-toroidal plane changes according to the array they belong to [26,27]. The complexity of the geometry requires the choice of a reference DWT layout. For this purpose, the second array was selected, that is the mid-one along the radial direction. It was considered sufficiently representative of the average geometrical features of all the DWTs present in the BRC.

BZ and FW inlet/outlet spinal water manifolds consist in rectangular channels running along the back of the segment, radially inwards with respect to the back supporting structure (see Section 2). They follow the SMS curved profile. In the TH model prepared, the design height difference between heat source and heat sink (the BZ OTSGs and the FW HEXs) thermal centers was maintained. This parameter is of primary importance in all the transients concerning natural circulation, such as LOFA. Manifold-simulating CVs are located before (inlet) and after (outlet) the ones modelling the DWTs/FW channels. In [2], the COB manifold layout is described. In a first approximation, this design was also used for the pipes simulating LOB/ROB and LIB/RIB segments. For any segment, CVs flow area was calculated to maintain the BZ and FW water manifolds inventory. CVs hydraulic diameter was evaluated based on the effective manifold layout.

The RELAP5 heat structure (HS) components were used in the input deck to accomplish several functions: account for the BB solid material inventories (tungsten and EUROFER97); simulate the breeder (simplifying the input); introduce the power source terms (heat flux and nuclear heating); represent the heat transfer phenomena taking place within the BRC; model the pipeline thermal insulation (for sector collectors/distributors and inlet/outlet FPs).

The lithium-lead flow path through the blanket was not modelled in this work from a hydrodynamic point of view. The breeder velocity inside the component is very low [2]. Within the BRC, where the thermal exchange between LiPb and DWTs/FW channels is significant, the breeder convective Heat Transfer Coefficient (HTC) was neglected and only the conductive heat transmission was considered, simulating the lithium-lead as a layer of structural material in the RELAP5 HS components.

A HS was used to simulate the FW front surface. A tungsten layer and a Eurofer thickness were modelled. The Eurofer thickness is the one between the plasma chamber and the FW cooling channels. The heat flux reported in [26] was applied as boundary condition for the plasma-facing surface. An average value was adopted since no poloidal differentiation was considered in the model. The radial segments of the FW component were simulated with a separate HS. In this case, only a Eurofer thickness was considered since the tungsten armor is present only in the front surface. To take into account the heat transfer between FW channels and DWTs inside the BRC, a HS was added. As already discussed, in the radial-toroidal plane, DWTs are divided into three arrays with different layouts. The same DWT reference layout chosen for the hydrodynamic model was used in

the thermal problem also. The radial distance between the FW cooling channels and the selected DWT is composed by: a first Eurofer layer, representing the FW thickness between FW cooling channels and FW internal surface; a LiPb layer, corresponding to the radial distance between the FW internal surface and the selected DWT layout; a second Eurofer layer, modelling the DWTs thickness. This HS allows to thermally couple the BZ and FW cooling circuits. Heat transfer between DWTs and LiPb inside BRC was also modelled with a dedicated HS. Two further HSs were used to account for the Eurofer inventory in the water and LiPb manifold region and in the back supporting structure, respectively.

Nuclear heating associated to the aforementioned HSs was computed thanks to the power density radial profiles presented in [27] and by considering the actual materials inventory distribution within the BRC. It was introduced in the input deck as an internal power source term, differentiated for each HS. For each sector, the batch of HSs described so far (six) was replicated for LOB/ROB, COB and LIB/RIB (for a total of 18).

The pipeline heat losses were modelled considering a constant containment temperature (30 °C), and a constant heat transfer coefficient (8 W/m^{2}K). A schematic view of the BB nodalization is provided in Figure 3. The model shown refers to only one of the sixteen identical toroidal sectors. For the correspondent hydrodynamic components, the figure reports also the identification numbers used in the input deck.

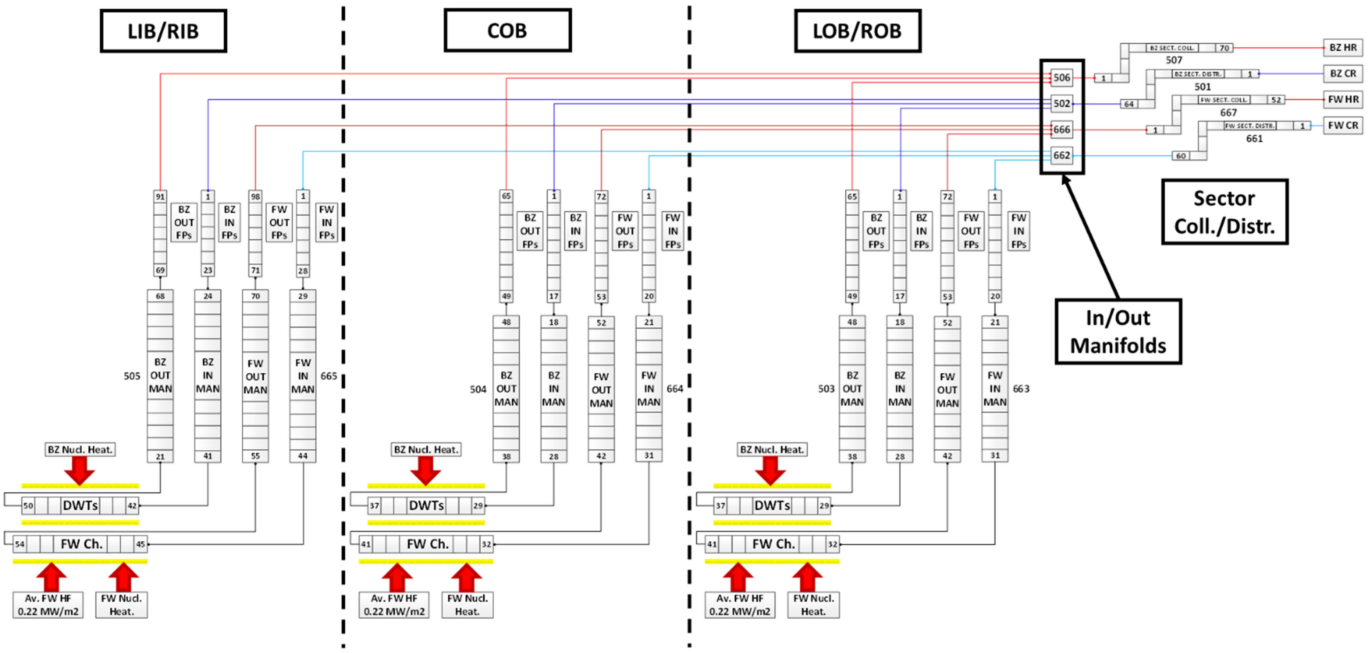

Figure 3. Schematic view of the blanket model, sector one of sixteen. All the Breeder Zone (BZ) and First Wall (FW) Primary Heat Transfer Systems (PHTS) in-vessel components are represented. In addition, red arrows indicate the power source terms.

3.2. PHTS Model

The routing of the BB PHTS pipelines was derived from the current CAD model [2,4,5]. K-loss coefficients for tees, elbows and area changes were calculated by using formulas in [28]. They were associated to pipe component internal junctions to correctly evaluate these minor head losses, when present. To each pipeline corresponds a RELAP5 pipe component, except for the hot and cold rings. For them, four pipes and two multiple junctions were used. Each pipe simulates a quarter of the ring (90°). One multiple junction component manages the connections between pipes (to close the ring) and between the rings and the hot/cold legs. The other multiple junction component links the hot/cold rings with the sector collectors/distributors. These connections are equally distributed

along the overall ring length to maintain the toroidal symmetry characterizing the DEMO reactor. Pipeline modelling is contained in Figures 4 and 5, respectively related to the BZ PHTS loop 1 and FW PHTS loop 1. An example of ring nodalization is shown in Figure 6. For the hydrodynamic components reported in each figure, the identification numbers used in the input deck are also indicated. Pipeline thermal insulation was modelled associating a heat structure to each pipe component. The external surface boundary condition for these HSs is the tokamak building atmosphere, modelled with a constant temperature and HTC, as already discussed in Section 3.1.

The BB PHTS pump system consists of six (four for the BZ and two for the FW) centrifugal single stage pumps. They are equally divided in the two loops constituting each PHTS. The MCPs were modelled by using RELAP5 pump components provided with a proportional-integral (PI) controller to set the design mass flow value.

The BZ OTSGs design foresees PHTS water flowing inside the tube bundle and PCS water flowing in shell side. A mesh length of 0.26 m was selected for these components in both (primary and secondary) sides. The details about the nodalization are reported in Figure 4.

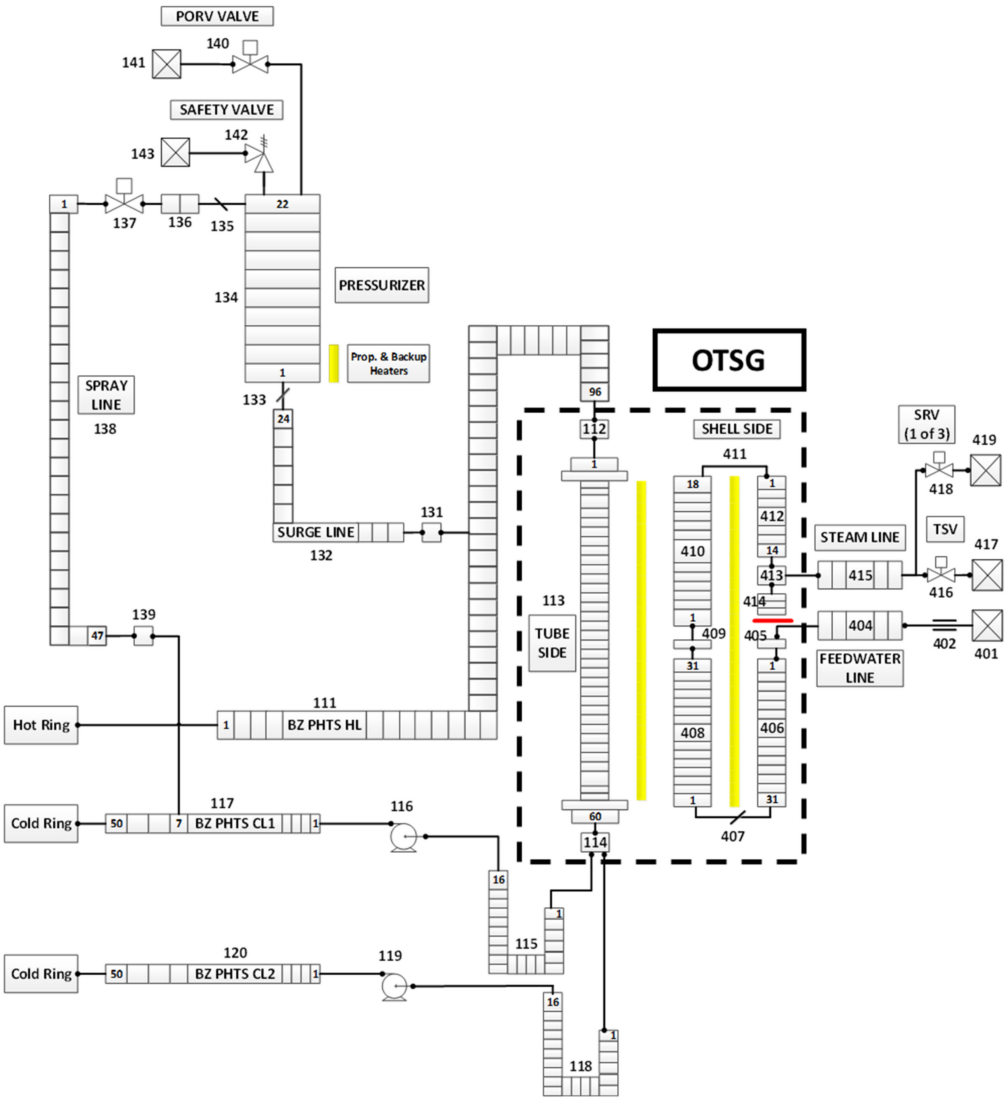

Figure 4. Schematic view of BZ PHTS model, loop one of two. Pressurizer system components are unique and connected only to the represented loop.

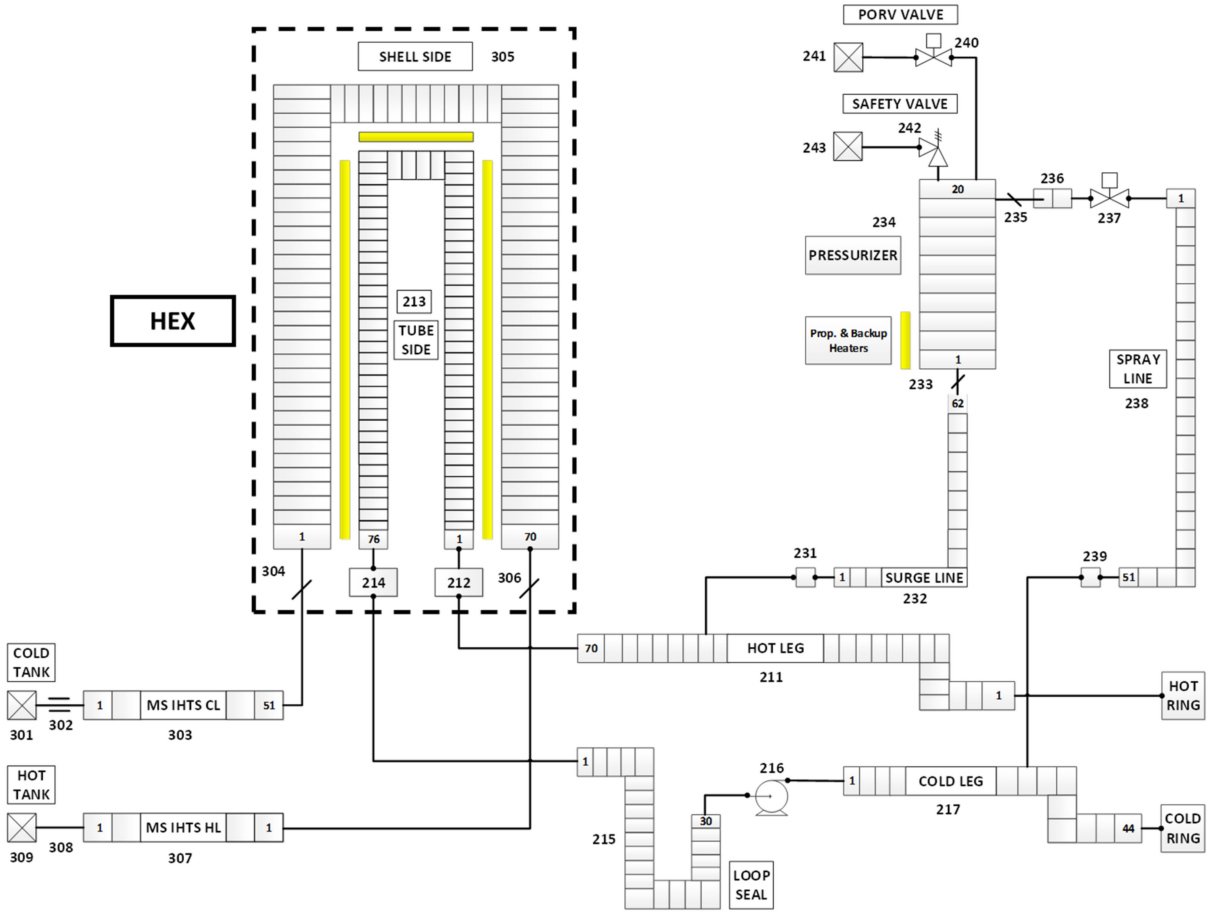

Figure 5. Schematic view of FW PHTS model, loop one of two. Pressurizer system components are unique and connected only to the represented loop.

Each OTSG is provided with two steam lines to avoid excessive pipeline pressure drops due to steam velocity. Feedwater line was simulated with a time-dependent volume and a time-dependent junction to set the PCS water inlet thermodynamic conditions, and with a pipe to simulate the pipeline section before the OTSG entrance. Steam lines were modelled up to the Turbine Stop Valves (TSVs) and equipped with steam line Safety Relief Valves (SRVs). PCS SRVs consists in three steps of relief valves provided with increasing setpoint: 90%, 95% and 100% of the PCS system design pressure (115% of the operating pressure reported in [4–6]). The step 1 relief valves were sized to discharge the 75% of the OTSG steam mass flow, considering chocked flow occurring in the valve throat section, while step 2 and step 3 to discharge the 37.5%. Hence, the full set of SRVs is able to discharge the overall OTSGs steam mass flow with an additional conservative margin of 50%. Main data related to PCS SRVs are collected in Table 1. A schematic view of the BZ OTSGs nodalization is shown in Figure 4. RELAP5 heat structures were used to simulate the thermal transfer taking place within steam generators, as well as the component heat losses. Furthermore, they allow to account for the OTSGs steel inventory (i.e., thermal inertia).

FW HEXs are pure countercurrent heat exchangers with PHTS water flowing inside tube bundle and IHTS molten salt flowing in shell side. The adopted CV length is 0.41 m. For each FW HEX, also the IHTS hot and cold legs were modelled. Cold leg was connected to a boundary condition to set the HITEC® inlet temperature and mass flow rate. The FW HEXs nodalization is shown in Figure 5. Also in this case, heat structures were used to simulate the heat transfer phenomena, the heat losses and the steel inventory related to each heat exchanger. The molten salt HTC was calculated with Sieder-Tate correlation, [29].

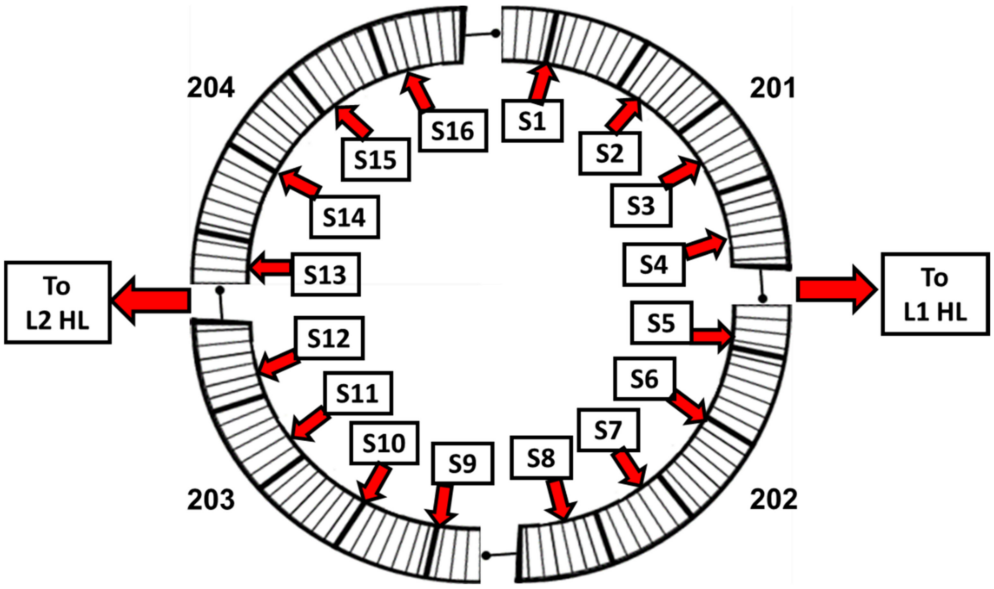

Figure 6. Example of ring nodalization, FW hot ring. The component connections with the sector collectors and loop hot legs are reported.

Table 1. Power Conversion System (PCS) steam line Safety Relief Valves (SRV) features.

Parameter	Unit	Step 1 SRVs	Step 2 SRVs	Step 3 SRVs
Throat section	m^2	1.80×10^{-2}	9.00×10^{-3}	7.50×10^{-3}
Area change rate [1]	s^{-1}	10	10	10
Opening setpoint	bar	66.4	70.0	73.7
Closing setpoint	bar	64.1	64.1	64.1

[1] Valve area change rate is the reciprocal of the valve opening/closing time.

The time-dependent junctions located on the BZ OTSGs feedwater lines and FW HEXs IHTS side cold legs were provided with temperature control systems. They are required to obtain the design PHTS water temperature at BB inlet [2,4–6]. The BZ OTSGs and FW HEXs designs were performed considering that they must exchange their nominal power when operating at End Of Life (EOL) conditions. For this, both tube fouling and tube plugging phenomena were taken into account. At Beginning Of Life (BOL) conditions, when no tube plugging and fouling factors are foreseen, the OTSGs and HEXs exchanged power exceeds the nominal value. This causes a significant alteration of the temperature field in the overall PHTS system and, in particular, at BB inlet. To keep the PHTS parameters at the design values in BOL condition, a control system is required. It was developed to ensure constant water thermodynamic conditions at BB inlet in any operational condition. PHTS temperature is read at OTSG outlet and then compared with a temperature target setpoint [2,4–6], producing an error. The error signal is scaled by using a PI controller. The controller output range goes from zero to 110% of rated PCS feedwater mass flow at EOL condition, [4–6]. The resulting output is the mass flow imposed by the time-dependent junction simulating the BZ OTSG secondary side inlet. The same control logic is applied to loop 2 OTSG and to both FW HEXs.

In each PHTS circuit, the pressurizer system guarantees the pressure control function, maintaining the water pressure at the required value independently on the temperature variations of the coolant induced by the pulsed plasma operation and, in general, by other transient conditions. The main component of this system is the steam bubble pressurizer (PRZ), connected to the loop 1 hot leg by means of a surge line. Since the water thermodynamic conditions are similar, for both BZ and FW PHTS, the pressurizer volume was scaled from PWR design, [30]. The scaling factor adopted was based on the ratios between circuit total inventories and reactor total thermal power. A further safety margin was

applied and the resulting component size increased. The tank and the surge line were both simulated with a pipe component. The associated heat losses were modelled with passive heat structures. The pressurizer is equipped with On/Off and proportional electric heaters and a spray line connected to the loop 1 cold leg and controlled by a valve. These systems are installed to face, respectively, under and overpressure transients occurring during both normal operations and abnormal conditions. The proportional heaters are set to operate in a range of pressure around the PHTS loop reference one. These heater banks are supplied by a varying input current that is a function of the pressure deviation signal. Normally, these components are energized at half current when pressure is at nominal value (null error), are cut off when this parameter reaches the higher setpoint and are at full power with pressure at lower setpoint. Instead, pressurizer backup heaters are normally de-energized heater banks turning on if pressure drops below the setpoint adopted for this component (lower than the one of the proportional heaters). They are simply on-off type with no variable control. The heaters electrical power was scaled from PWR design, [30], by using a scaling factor based on reactor thermal power and applying a safety margin. Pressurizer heaters were simulated with active heat structures. The spray valve controller is set to modulate the valve flow starting from a lower setpoint up to a higher one correspondent to the fully open status. Pressurizer sprays operate to prevent lifting of the relief valve. The cold leg water admitted through these components is extremely effective in limiting pressure increases during transient or accident conditions. The correspondent flow capacity was sized by scaling from PWR design [30]. The surge line and spray line routing was derived from CAD model [2,4,5], and rigorously maintained. In case of abnormal transients, if spray nozzles fail in reducing pressure, at the top of pressurizer is also foreseen the presence of a Pilot (Power)-Operated Relief Valve (PORV) and an SRV. A dedicated line connects these components to the pressure relief tank, allowing the discharge of steam. The PORV is provided for plant operational flexibility and for limiting the number of challenges to the pressurizer SRV. For this reason, the former is provided with a lower setpoint than the latter. PORV and SRV were modelled with RELAP5 valve components.

The overall nodalization used for BB PHTS pressurizer system is shown in Figures 4 and 5, for BZ and FW, respectively. The main design data related to both BZ and FW PHTS pressurizer systems are contained in Table 2. The pressure control function setpoints, chosen considering the PWR design [31], are gathered in Table 3.

Table 2. BZ and FW PHTS pressurizer system features.

Parameter	Unit	BZ PHTS	FW PHTS
Pressurizer volume	m^3	101.5	39.3
Proportional heater bank power	kW	1200	800
On/Off heater bank power	kW	2400	1600
Spray line flow capacity	kg/s	36.2	17.9
PORV throat section	m^2	1.84×10^{-3}	1.52×10^{-3}
SRV throat section	m^2	1.84×10^{-3}	1.52×10^{-3}
PORV/SRV area change rate [1]	s^{-1}	10	10

[1] Valve area change rate is the reciprocal of the valve opening/closing time.

Table 3. BZ and FW PHTS pressure control function.

Parameter	Unit	BZ PHTS	FW PHTS
Reference Pressure	bar	155	155
Proportional heater bank lower setpoint	bar	154	154
Proportional heater bank higher setpoint	bar	156	156
Back-Up heater bank on/off setpoint	bar	154	154
Spray Valve start opening setpoint	bar	157	157
Spray valve fully open setpoint	bar	160	160
PORV valve opening setpoint	bar	170	170
PORV valve closing setpoint	bar	165	165
SRV opening setpoint	bar	178	178
SRV closing setpoint	bar	173	173

4. Results

4.1. Full Plasma Power State

The RELAP5 model described so far was used to perform a steady-state simulation of full plasma power state at Beginning Of Life (BOL) condition. During DEMO normal operations, this is the most challenging scenario for the BB PHTS, as confirmed by results presented in [14]. For this reason, such state was chosen as initial condition for the accidental transient calculations discussed in the following sections. The full thermal-hydraulic characterization of BZ and FW primary cooling systems during this scenario is reported in Table 4. The parameters with the indication "BC" were imposed as boundary conditions for the calculation. The mass flow and temperature control systems implemented in the input deck are able to guarantee the required thermodynamic conditions at the BB inlet. Table 4 also indicates the pump head provided by MCPs and the power terms associated with each PHTS. Simulation outcomes are in good accordance with reference data derived from [2,4–6]. Minor discrepancies in the OTSGs/HEXs secondary side parameters are due to the fact that the sizing of these components was performed at EOL, as discussed in Section 3.2. A time step sensitivity was carried out, varying this parameter from 1.0×10^{-3} s to 1.0×10^{-2} s. No sensible differences were observed in the results. Values in Table 4 are for a time step of 5.0×10^{-3} s.

Table 4. Full plasma power state: main thermal-hydraulic parameters related to BZ and FW PHTS, Intermediate Heat Transfer System (IHTS) and PCS. Comparison between simulation results and reference data derived from [2,4–6].

	Parameter	Unit	BZ PHTS		FW PHTS	
			Simulation Result	Reference Data	Simulation Result	Reference Data
PHTS	Mass Flow (per MCP)	kg/s	1915.6	1915.6	1136.8	1136.8
	Hot Leg Temperature	°C	328.2	328	328.1	328
	Cold Leg Temperature	°C	295	295	295	295
	MCP Head	MPa	0.94	0.95	0.83	0.84
	PRZ pressure	MPa	15.6	15.5	15.6	15.5
PCS/IHTS	Feedwater/HITEC® Mass Flow	kg/s	392.8	404	2955.6	3524
	Feedwater/HITEC® Inlet Temp. (BC)	°C	238	238	280	280
	Steam/HITEC® Outlet Temperature	°C	314.6	299	327.7	320
Power Terms	Power removed from blanket	MW	1482.4	1483.2	438.3	439.8
	Power exchanged at OTSG/HEX(per component)	MW	744.5	741.6	219.8	219.9
	MCPs Total Power	MW	11.9	12.1	3.0	3.2
	PRZ Heaters Power	MW	1.08×10^{-2}	-	4.87×10^{-3}	-
	Total System Heat Losses	MW	0.6	-	0.45	-

4.2. Transient Analysis

4.2.1. Selected Cases

The BB PHTS response during accidental conditions was investigated. The calculations are system analyses aimed at understanding the primary cooling circuits TH behavior during such transients. As previously stated, full plasma power state was used as initial condition. The selected PIEs are partial and complete Loss of Flow Accident (LOFA). These accidental scenarios were studied when occurring in both BZ and FW PHTS. Simulations were replicated also considering the influence of loss of off-site power, occurring in combination with PIE. The matrix of all the transient simulations performed in the framework of the current computational activity is represented in Table 5.

Table 5. Matrix of transient simulations performed.

Case ID	PIE	System Involved With PIE	Loss of Off-Site Power [Yes/No]
LF1	Partial LOFA	FW PHTS	no
LF2	Complete LOFA	FW PHTS	no
LF3	Partial LOFA	BZ PHTS	no
LF4	Complete LOFA	BZ PHTS	no
LF5	Partial LOFA	FW PHTS	yes
LF6	Complete LOFA	FW PHTS	yes
LF7	Partial LOFA	BZ PHTS	yes
LF8	Complete LOFA	BZ PHTS	yes

4.2.2. Selected Boundary Conditions and PHTS Actuation Logic

The LOFA PIE is the partial or complete loss of primary coolant flow in BZ or FW PHTS, according to the case considered (see Table 5). Primary pumps coast-down is ruled by the torque-inertia equation reported below.

$$T_{em}(\omega) - T_{hyd}(\omega) - T_{fr}(\omega) = I \cdot d\omega/dt \quad (1)$$

In the previous equation, $T_{em}(\omega)$ is the motor electromagnetic torque, that during coast-down is zero, $T_{hyd}(\omega)$ is the hydraulic torque due to system pressure drops, $T_{fr}(\omega)$ is the pump frictional torque due to losses inside the MCP component, ω is the rotational velocity and I is the pump moment of inertia. In the framework of Work Package Balance Of Plant 2020 computational activity, [14], a complete LOFA in both BZ and FW systems (worst possible scenario) was studied. The analysis was aimed at evaluating the required flywheel to be added to BB MCPs in order to obtain the best PHTS and blanket TH performances during the accidental evolution. For this reason, a sensitivity was carried out on this parameter. The selected values for pump moment of inertia were: 3000 kg·m^2 for BZ MCPs and 1573 kg·m^2 for FW MCPs (case 4 in [14]). These parameters were adopted for all the transient simulations involved in the current transient analysis.

An actuation logic, involving some components of the DEMO reactor, was proposed and preliminary investigated. It is inspired by the one used for Generation III + nuclear power plants. The following features were implemented:

- Plasma termination (PT) is actuated by one of the following signals: (i) low flow on BB MCPs (<80% of rated value); (ii) high pressure on BB PRZs (>167 bar); (iii) high temperature at BZ/FW outlet FPs (2 °C below the saturation temperature at the PHTS reference pressure).
- Turbine Trip (TT) is triggered by one of the following signals: (i) PT signal; (ii) low steam flow at OTSGs outlet (<85% of rated value); (iii) low steam temperature at OTSGs outlet (2 °C above the saturation temperature at the PCS reference pressure).
- TT is followed by: (i) PCS feedwater ramp down; (ii) TSVs closure.
- PHTS pressurizer heaters are cut off: (i) on low-level signal in BB PRZs; (ii) following TT signal.

- Spray line flow is interrupted only when all the MCPs belonging to a primary cooling system are off. The hypothesis is that redundant spray lines are connected to both PHTS loops.

The margin adopted for the temperature signals was selected to take into account the typical uncertainty related to a thermocouple reading. For what concerns the BB MCPs trip, different strategies were considered whether or not the loss of off-site power is assumed. If not, for a BZ or FW primary pump, MCP trip can occur following: (i) PIE event; (ii) high-temperature signal at pump inlet (5 °C below the saturation temperature at the PHTS reference pressure). The margin was chosen to avoid cavitation in the component in any transient scenario. If loss of off-site power is assumed, to the previous conditions it is also added the TT signal, since, in this scenario, the turbine is the only element ensuring the Alternating Current (AC) power needed for the MCPs operation. The PI controller associated to BZ and FW primary pumps and used in the full plasma power steady-state simulation is disabled. The rotational velocity is imposed as a constant boundary condition until the MCP trip is not triggered. From this moment, the component coast-down is ruled by the torque-inertia equation reported above.

Also, the management strategy for MS IHTS mass flow was differentiated according to the presence or not of off-site power. If available, HITEC® mass flow is ramp down 10 s after the PIE. Conservatively, it is assumed that the PIE occurs at the end of plasma pulse when the ESS cold tank is nearly empty. Hence, also the HITEC® mass flow must be stopped shortly after the Start Of Transient (SOT). If off-site power is lost, IHTS mass flow is ramp down also following the TT signal (the previous condition is still used). In fact, in this scenario, the turbine is the only element ensuring the AC power needed for the molten salt pumps operation.

The temperature control systems adopted for the full plasma power scenario and related to PCS feedwater and IHTS mass flow are disabled. These parameters are imposed by means of time-dependent junctions and respond to the actuation logics previously described. As a preliminary tentative, their ramp-down is simulated with a linear trend going from nominal value to zero in 10 s. Steam line TSVs are supposed to close in 0.5 s. The plasma ramp-down curve is derived from [32] and reported in Table 6. The relative trend should be applied to both nuclear heating and incident heat flux. It lasts 42 s, after which only decay heat is left (nearly 1% of the reactor rated power).

Table 6. Plasma ramp-down curve: tabulation of relative power values vs time.

Time from Plasma Shutdown [s]	Rel. Power [1] [–]	Time from Plasma Shutdown [s]	Rel. Power [–]
0	1.000	26	0.382
2	0.943	28	0.348
4	0.887	30	0.315
6	0.832	32	0.284
8	0.779	34	0.256
10	0.728	36	0.229
12	0.678	38	0.205
14	0.631	40	0.182
16	0.584	42 [2]	0.162
18	0.540	44	0.019
20	0.498	45	0.017
22	0.457	1 h	0.009
24	0.419	1 day	0.002

[1] Relative values refer to nominal power in full plasma power state. [2] This is the end of the ramp down curve. Next value belongs to decay heat trend.

The initiating event occurs after 100 s of full plasma power state (grey background in the figures of Sections 4 and 5). Timeline was reset in the plots to have PIE at 0 s. Transient calculation was run for 9000 s (2.5 hr), for an overall simulation time of 9100 s. Different time steps were adopted in the calculation. In the first part of the transient, when thermal

excursions are expected to be more significant, a lower time step was used (5.0×10^{-3} s). In the final part, this parameter was increased (1.0×10^{-2} s) to speed up the simulation.

4.2.3. LOFA Transients Involving FW Cooling Circuit

FW System Transient Evolution

After PIE, FW PHTS primary flow starts to decrease. In LF1 and LF5 cases, initiating event involves only loop 1 MCP (partial LOFA), instead, in LF2 and LF6 sequences, both loop pumps are stopped (complete LOFA). Low flow is detected shortly after the SOT and plasma termination is triggered. Consequently, also turbine trip is actuated. In LF5 scenario, where loss of off-site power is assumed, this causes the stop of the loop pump not interested from PIE. For this reason, in LF2, LF5 and LF6 transients, the coast-down of both loop pumps is nearly contemporaneous and these cases have a quite similar accidental evolution. Case LF1 differs from the others since loop 2 MCP continues to provide primary flow up to nearly the End of Transient (EOT). A summary of the transient calculations characterized by PIE involving FW pumps is offered by Table 7.

Table 7. Summary table for Loss of Flow Accidents (LOFA) involving FW PHTS Main Coolant Pumps (MCPs).

Event/Parameter	Unit	LF1	LF2	LF5	LF6
PIE (LOFA)	-	Partial (FW)	Complete (FW)	Partial (FW)	Complete (FW)
Loss of off-site power	yes/no	no	no	yes	yes
PT signal occurrence	s	1.5	1.5	1.5	1.5
TT signal occurrence	s	1.5	1.5	1.5	1.5
TSVs start to close	s	1.5	1.5	1.5	1.5
Start of PCS feedwater ramp-down	s	1.5	1.5	1.5	1.5
Start of IHTS mass flow ramp-down	s	10	10	1.5	1.5
Time of FW PHTS water temperature peak	s	15	24	23	23
FW PHTS water temperature peak [1]	°C	329	332	332	332
Time of BZ PHTS water temperature peak	s	-	-	60	60
BZ PHTS water temperature peak [1]	°C	-	-	339	339
FW MCP Trip occurrence (pump not interested by PIE)	s	7696	-	1.5	-
BZ MCPs Trip occurrence	s	7112	7084	1.5	1.5
Time to evacuate BZ OTSGs secondary side inventory	s	500	500	2200	2200
Water mass discharged from BZ OTSGs sec. side	kg	13,281 (per OTSG)	14,718 (per OTSG)	12,795 (per OTSG)	15,465 (per OTSG)
FW PORV first opening time (Long Term)	s	7344	1284	2200	1988
Total FW PHTS water mass discharged at EOT	kg	1301	2094	1398	1352
BZ PORV first opening time (Long Term)	s	6776	6736	4512	4192
Total BZ PHTS water mass discharged at EOT	kg	6724	5831	5482	4417

[1] For all the sixteen sectors, both the BZ and FW PHTS water temperatures were detected at the outlet of COB segment. For each PHTS, peak temperature reported in the table is the maximum among all the temperature readings.

Case LF1

As already stated, loop 2 MCP continues to provide primary flow. The transient results dissymmetrical with respect to the toroidal dimension. The sixteen sectors experience different flows (Figure 7a), with higher values in the ones nearest to the active pump. Consequently, also the PHTS temperatures at BB inlet/outlet are differentiated. Figure 7b reports the values referred to all sixteen sectors. COB segment was chosen as reference to plot simulation results. Forced flow due to loop 2 MCP significantly smooths the temperature peak at BB outlet. The maximum increase (associated to the sectors nearest to the failed pump) is of only one degree (Table 7) with respect to rated value. The temperature excursion is quite negligible.

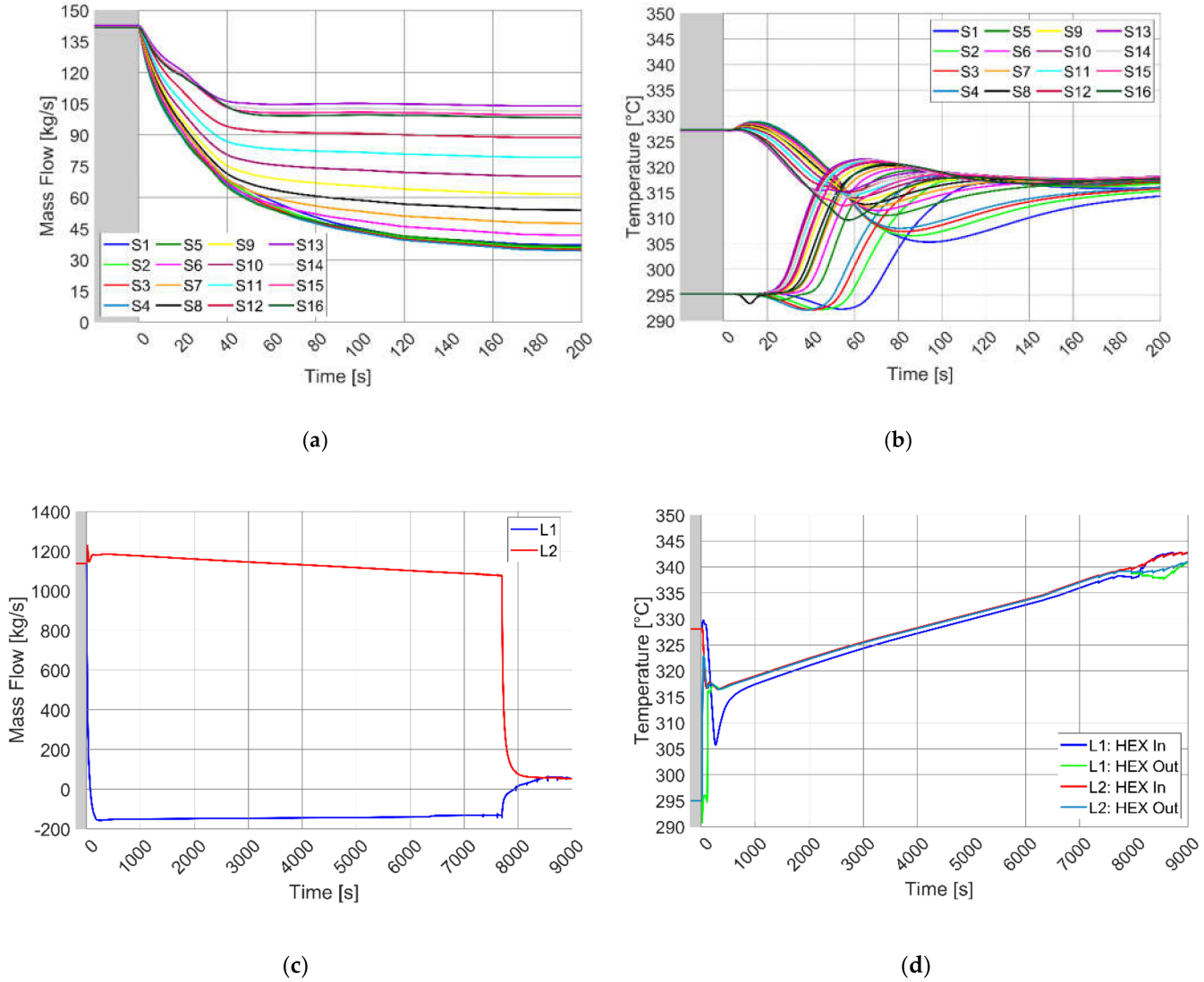

Figure 7. Partial LOFA on FW PHTS without loss of off-site power (LF1 transient): (**a**) Mass flow in FW sectors (early time); (**b**) FW PHTS water temperatures at BB inlet & outlet (all sectors, early time, COB segment); (**c**) Mass flow elaborated by FW PHTS MCPs (full range); (**d**) FW PHTS water temperatures at Heat EXchangers (HEXs) inlet & outlet (full range).

Another interesting effect is the flow inversion in loop 1 (negative mass flow in Figure 7c). The pressure drops related to the blanket component are so high that a part of the flow provided by loop 2 MCP goes through loop 1 in reverse direction instead of flowing in the BB sectors. The reverse flow also causes a temperature inversion in the correspondent loop. After the trip of loop 2 pump (Figure 7d and Table 7), forced circulation is lost and the establishment of natural circulation restores the original temperature field in

loop 1. Instead, in the other loop, the forced circulation provokes a quick convergence of the system temperatures. Later, they start to positively drift since BB decay heat overwhelms the system heat losses. The temperature slope is of nearly 12 °C/hr (25 °C in 7500 s). In the case of forced circulation (LF1), the curve slope is higher than the one associated to sequences dominated by natural circulation (LF2, LF5 and LF6, Figure 9c). This can be justified considering that the PHTS coolant is also heated by pumping power. This contribute is of the same order of magnitude of the decay heat. Once loop 2 pump is stopped, when forced circulation is lost and natural circulation establishes, if simulation time were increased, the temperature slope for LF1 scenario would become the same as other transients.

For what concerns the FW PHTS pressure, the presence of the forced circulation (even if reduced with respect to rated value) avoids the challenging of PRZ PORV at SOT (Figure 8a). In the mid-long term, since loop 2 pump is active also pressurizer sprays are still available. The system pressure is kept constant for a long time interval (Figure 8b). During it, with the increase of the system temperature, spray intervention in reducing pressure becomes less and less effective. In fact, from time to time, they introduce in the pressurizer control volume water at higher enthalpy. The level in the component increases almost linearly, as shown in Figure 8c. At a certain point, sprays are unable to perform the pressure control function and the system pressure start to rise triggering the PORV (Figure 8b, for the timing see Table 7). The valve opens when the pressurizer is nearly solid (Figure 8c). From this moment, pressure in the PHTS follows a sawtooth trend due to the PORV periodical openings. This is the way used by FW system to dissipate the decay heat produced in the BB. The total water mass discharged from FW PHTS at EOT is reported in Table 7.

The trend of the maximum Eurofer temperature in the FW component is shown by Figure 8d. After plasma shutdown, the material temperature drops driven by PHTS water temperatures. Instead, in the mid-long term, FW component is heated up by the decay heat and experiences the same temperature slope of PHTS water.

Cases LF2, LF5 and LF6

The FW PHTS mass flows through blanket sectors follow the pump coast-down. It is shown for LF6 sequence in Figure 9b. For all the considered accidental scenarios, as already discussed before, the coast-down of both MCPs is nearly contemporaneous. Hence, these transients result symmetrical with respect to the toroidal dimension. This is clearly visible in Figure 9a reporting the FW PHTS temperatures at BB inlet/outlet (COB segment). Values are plotted for all the sixteen sectors, with a single color for each case considered. Outlet temperatures experience a slight increase due to the short time interval between the occurrence of PIE (i.e., start of pump/pumps coast-down) and the detection of PT signal. After that, since pump coast-down advances more slowly than plasma shutdown (Table 6), outlet temperatures decrease. Peak temperature is the same for all the sectors and for all the cases (Table 7). In LF5 and LF6 scenarios, where loss of off-site power is assumed, IHTS mass flow is ramp down following the turbine trip, while in LF2 sequence it is available for the first 10 s of the transient. As a result, in this latter case, BB inlet temperatures initially decrease (Figure 9a) and restart to increase only after the mass flow ramp down. Instead, in LF5 and LF6 transients, they start immediately to increase, since secondary flow is lost shortly after the SOT. However, apart from this initial difference, the inlet temperatures have a quite similar trend for all the cases.

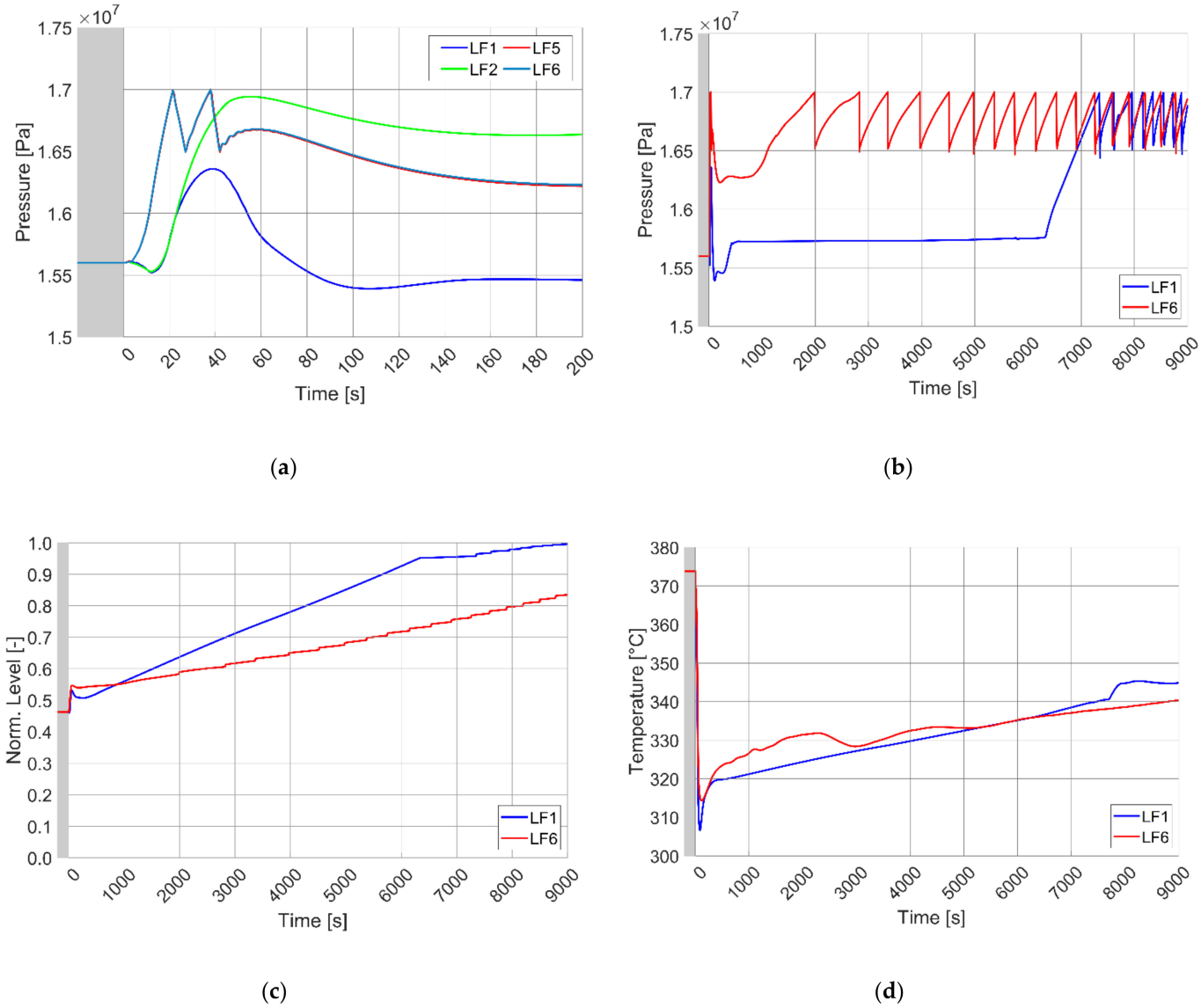

Figure 8. Comparison between LF1 and LF6 transients: (**a**) Pressure in FW PHTS (early time); (**b**) Pressure in FW PHTS (full range); (**c**) Collapsed level in FW pressurizer (normalized, full range); (**d**) Maximum Eurofer temperature in FW component (full range).

The loss of the heat sink also produces a sudden increase in the FW PHTS pressure, as shown by Figure 8a. For LF5 and LF6 sequences, the pressure rise is managed by the PRZ PORV. Instead, in LF1 and LF2 scenarios, the availability of the IHTS mass flow avoids the opening of this component. In the long term, referring to FW PHTS parameter trends, no sensible differences are detected between cases LF2, LF5, LF6. For this reason, only results associated to LF6 sequence were plotted in the figures reported in this section.

During FW pump coast-down system reaches a quite uniform temperature (Figure 9c). It takes a long time interval before the natural circulation establishes in the system. During it, FW temperatures also experience an inversion. Once the natural circulation is completely established, FW temperatures start to positively drift due to the residual decay heat produced in the blanket. The system heat losses are not able to counterbalance this source term. The PHTS temperatures rise of 10 °C in the last 4000 s of simulation with a slope of nearly 9 °C/hr. As discussed before, this parameter is lower than the one observed for case LF1.

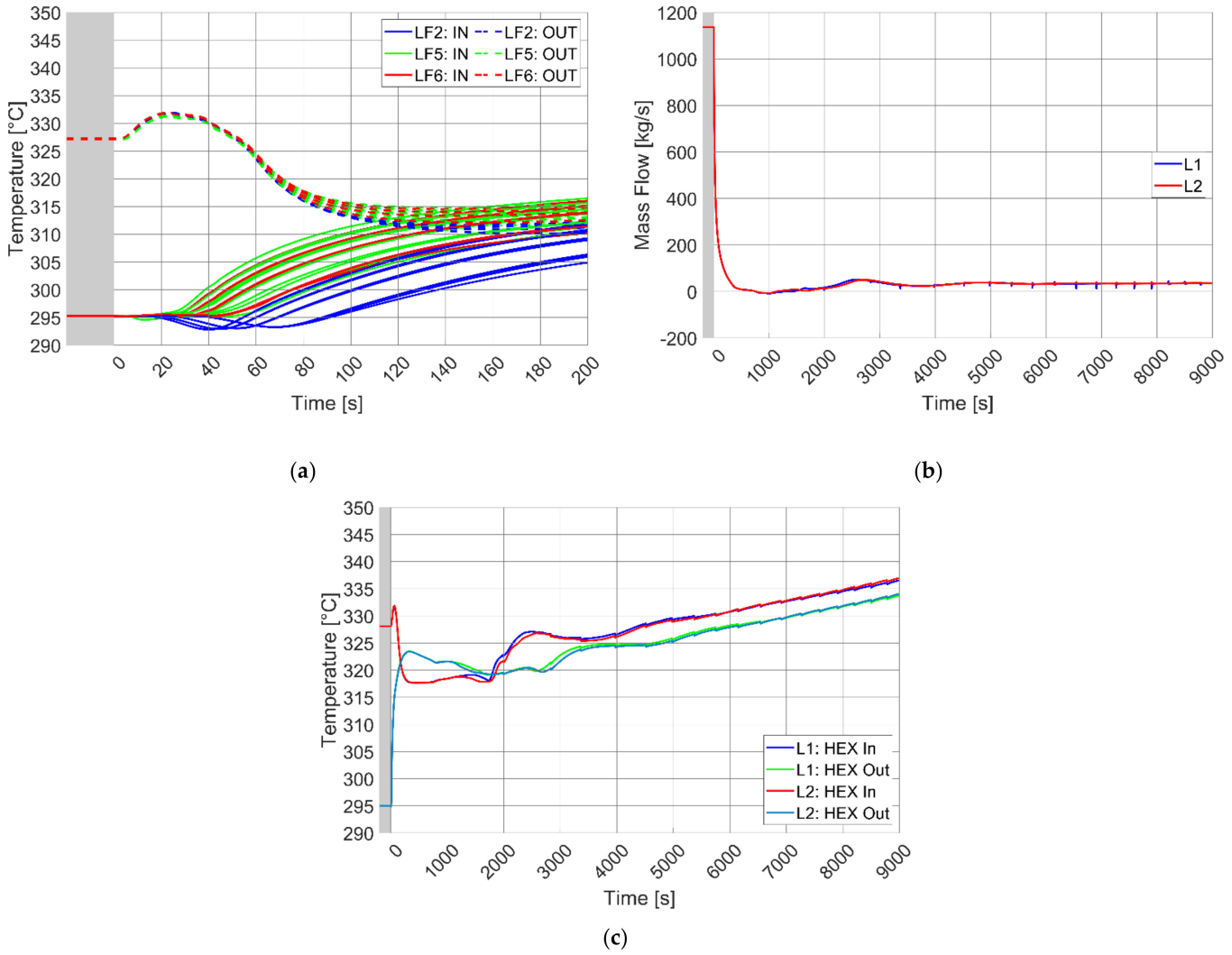

Figure 9. Parameter trends in FW PHTS for LOFA transients characterized by natural circulation (LF2, LF5, LF6): (**a**) FW PHTS water temperatures at BB inlet & outlet (all sectors, early time, COB segment); (**b**) Mass flow elaborated by FW PHTS MCPs (full range, only LF6); (**c**) FW PHTS water temperatures at HEXs inlet & outlet (full range, only LF6).

During accidental evolution, pressure in FW PHTS system increases (Figure 8b). Pressurizer sprays are disabled since all the system pumps are off. Pressure rise continues up to the PORV opening setpoint. With respect to LF1 sequence, the timing of this event is significantly anticipated (Table 7). Later, the system pressure begins to cycle accordingly with the valve component multiple openings. Discharging mass through the PORV is the way adopted by the FW system to dissipate the decay heat produced in the BB. The total amount of water evacuated from FW PHTS at EOT is reported in Table 7. The level in the pressurizer is shown in Figure 8c, normalized with respect to the total height of the component. Pressure rise produces a continuous mass insurge (i.e., level increase) in the component. Furthermore, a step up in the water level is experienced any time PORV opens to discharge mass. At EOT the component is nearly solid.

Finally, Figure 8d reports the trend of the maximum Eurofer temperature in the FW component. The peak present in the PHTS water BB outlet temperatures (Figure 9a) is not visible in the material temperature trend. The FW thermal inertia, even if low, completely smooths this temperature excursion. In the long term, the trend follows that of the PHTS water.

BZ System Transient Evolution

The BZ PHTS performances are strongly influenced by the presence of off-site power. If available, as in LF1 and LF2 sequences, system pumps continue to provide primary flow (Figure 10d is referred to loop 1 MCP 1). Among the interested cases, LF1 was selected to represent the scenarios characterized by the presence of off-site power and only its parameters are plotted in the following figures. Initially, a continuous slight decrease can be detected in the flow trend. It is due to the rise of system average temperature. This causes the decrease of water density in the pump component and also an increase of the loop pressure drops. These two combined effects produce the reduction of the mass flow elaborated by BZ MCPs. When the temperature at pump inlet reaches the setpoint, MCPs trip occurs and forced circulation is lost (for the timing see Table 7). If loss of off-site power is assumed, as in LF5 and LF6 scenarios, BZ MCPs trip occurs following the turbine trip and forced circulation is lost shortly after the SOT (Figure 10d). Natural circulation establishes in the BZ system. LF6 was selected as reference case to plot simulation results related to the absence of off-site power. The presence or not of the forced circulation is the main element affecting the BZ PHTS behavior during such transients.

Forced Circulation (LF1 and LF2 Cases)

When plasma shutdown and turbine trip are triggered, BZ system loses the power source (plasma pulse) and the heat sink (PCS feedwater) at the same time, while maintaining primary flow at nearly nominal value. This combination of factors produces the convergence of the system hot and cold temperatures to a common value (Figure 10a). No temperature peak is detected at BB outlet in any sector. Figure 10a is related to COB segment, but this is still valid for LOB/ROB and LIB/RIB.

The plasma shutdown takes more time (nearly 40 s, Table 6) with respect to PCS feedwater ramp down (10 s) and, above all, TSVs closure (0.5 s). This leads to a power unbalance and a consequent pressure spike in both BZ PHTS and PCS. In BZ PHTS, Figure 10b, the power surplus is dissipated by multiple openings of the pressurizer PORV. In the same way, the PCS pressure transient is managed by the steam line SRVs (Figure 10c). All three steps of this valve system are forced to intervene to limit the pressure increase. The maximum value experienced is slightly above the PCS design pressure. This demonstrates the appropriateness of the current valve design.

In the mid-term, BZ system is cooled down by the OTSGs (Figure 10e, related to BZ loop 1). Their residual cooling capability is due to the flow circulating in the steam generators any time the SRVs open to reduce the PCS pressure. This cooling system is available until a significant water inventory is present in the OTSGs secondary side. As shown by Figure 10f (loop 1 OTSG), the water level in the steam generator riser drops to zero at SOT in correspondence with the power surplus due to plasma shutdown. After that, water level is still present only in the lower downcomer. This is the water inventory available in the mid-term at the OTSGs secondary side. Any time SRVs open to reduce PCS pressure, level decreases. Once the lower downcomer has been completely evacuated, (for the timing and the total amount of mass discharged see Table 7), the dominant effect on the BZ temperatures is the presence of the decay heat. System heat losses are unable to dissipate such thermal power. Temperatures start to positively drift (Figure 10e) with a slope of nearly 12 °C/hr (22 °C in 6500 s, from 500 s to 7000 s). Even for the BZ system, the curve slope related to the forced circulation (LF1 and LF2 sequences) is higher than the one associated to cases dominated by natural circulation (LF5 and LF6). The difference is due to the pumping power, acting as an additional source term of the same order of magnitude of the decay heat. After BZ MCPs trip, whose timing is reported in Table 7, when forced circulation is lost and natural circulation establishes, if simulation time were increased, the same temperature slope would be observed for all the cases.

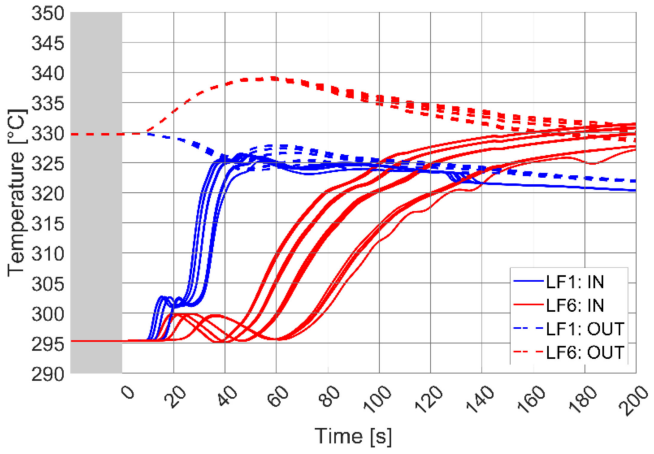

(**a**)

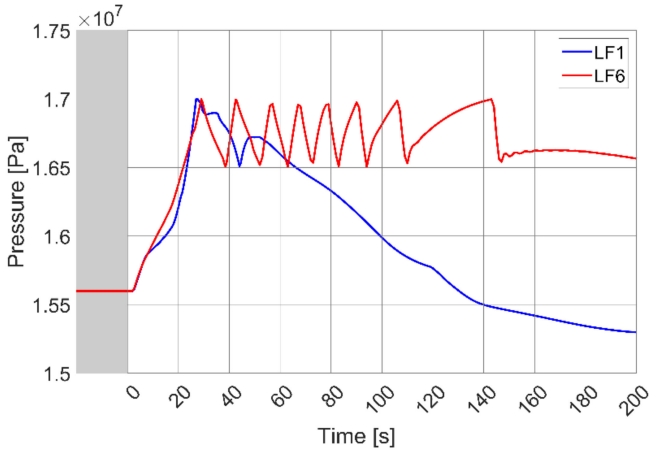

(**b**)

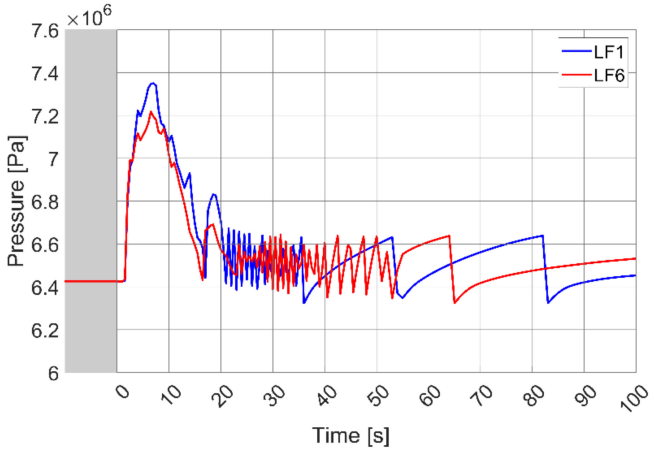

(**c**)

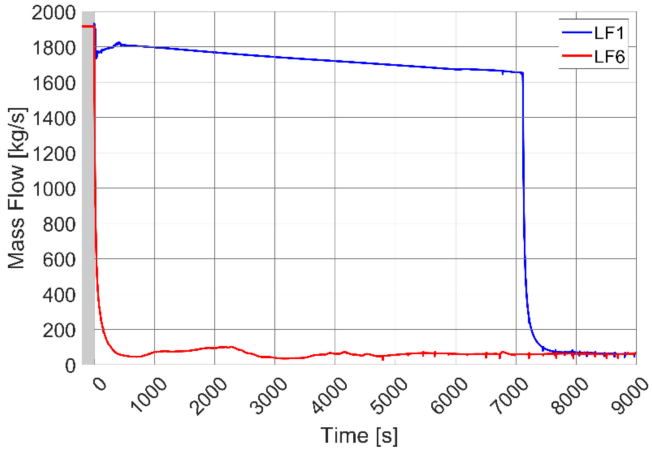

(**d**)

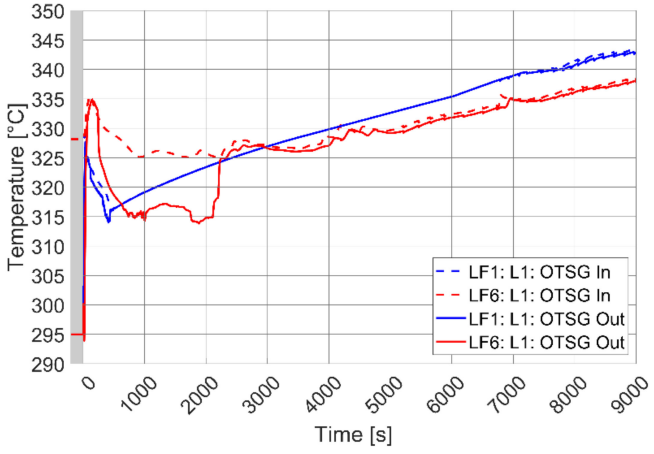

(**e**)

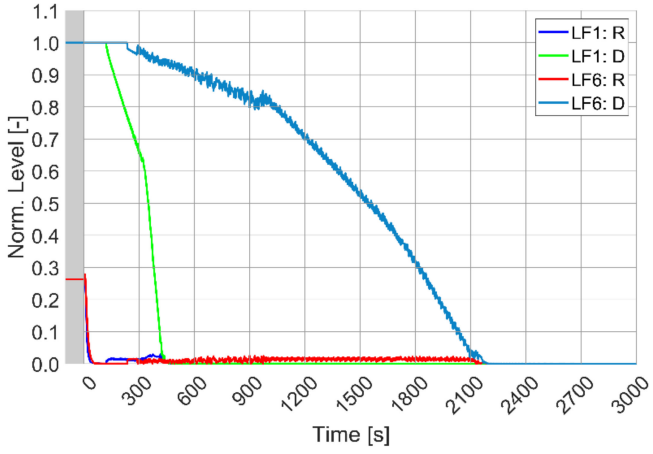

(**f**)

Figure 10. *Cont.*

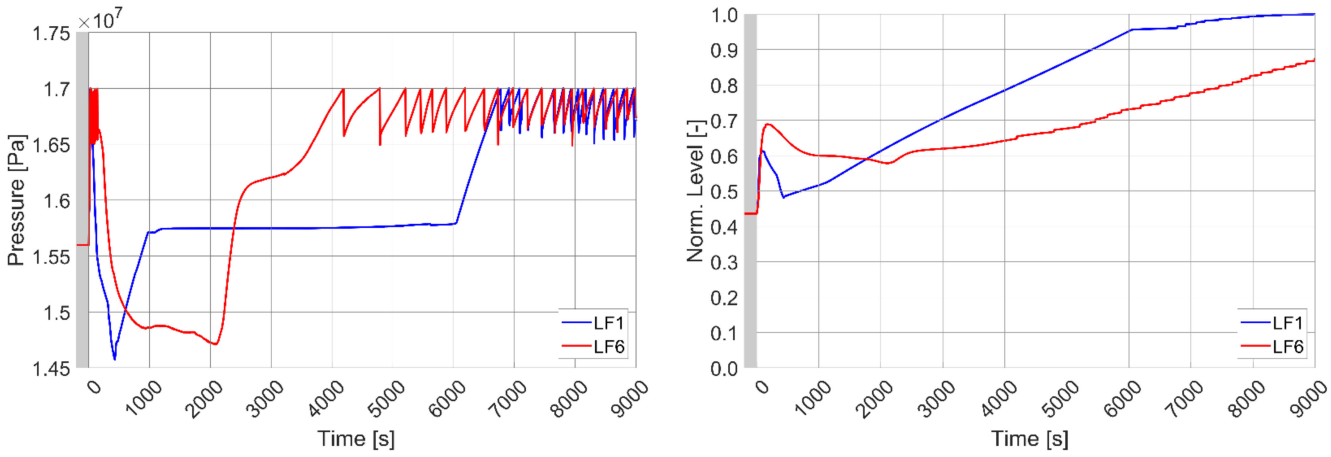

(**g**) (**h**)

Figure 10. Comparison between LF1 and LF6 transients: (**a**) BZ PHTS water temperatures at BB inlet & outlet (all sectors, early time, COB segment); (**b**) Pressure in BZ PHTS (early time); (**c**) PCS pressure at OTSGs secondary side outlet (early time); (**d**) Mass flow elaborated by BZ loop 1 MCP 1 (full range); (**e**) BZ PHTS water temperatures at OTSG inlet & outlet (loop 1, full range); (**f**) Collapsed level in loop 1 OTSG secondary side riser (R) and lower downcomer (D) (normalized, full range); (**g**) Pressure in BZ PHTS (full range); (**h**) Collapsed level in BZ pressurizer (normalized, full range).

The BZ pressure goes down during the cooling transient provided by the OTSGs in the mid-term (Figure 10g). Its value drops even below the nominal one. This is possible because the pressurizer heaters are offline due to turbine trip. After the complete blowdown of OTSGs secondary side inventory, the system pressure rise following the temperature trend. This increase is limited by the pressurizer sprays that are still active since their operation depends on the BZ pumps. With the increase of the system temperature, they introduce in the pressurizer control volume water at higher enthalpy, reducing the effectiveness of their pressure control action. The pressurizer level also increases almost linearly during this time interval. It is reported in Figure 10h normalized with respect to the component height. When the pressurizer is nearly solid, sprays are unable to perform the pressure control function and the system pressure restart to rise, triggering the PORV. The timing of this event is in Table 7. From this moment, PHTS pressure starts to cycle. In this way, PORV component dissipates the decay heat produced in the blanket. The total PHTS mass discharged at EOT is shown in Table 7.

Natural Circulation (LF5 and LF6 Cases)

In these cases, with PT and TT signals, also the BZ MCPs trip is triggered. The BZ system loses at the same time: the power source (plasma shutdown), the heat sink (turbine trip) and the primary flow (MCPs trip). The PHTS water temperature trends at BB inlet/outlet (Figure 10a, COB segment) result from the relative balance between these decreasing parameters. Initially, the plasma power is dominant and a temperature spike can be detected at the blanket outlet. The peak value is reported in Table 7. Then, the primary pump coast-down, which lasts more than the plasma shutdown curve, becomes prevalent and the system temperatures converge.

The initial power surplus produces a pressure spike in both BZ PHTS and PCS. In the former, Figure 10b, it is managed by the pressurizer PORV, while in the latter, Figure 10c, the pressure transient is limited by the steam line SRVs. All three steps are necessary to limit the pressure rise. The observed maximum value is slightly above the PCS design pressure, proving the effectiveness of the SRVs design even in these scenarios.

In the mid-term, BZ system is cooled down by the OTSGs, as shown in Figure 10d regarding loop 1. As already discussed, their residual cooling capability is available until a significant water inventory is present at OTSGs secondary side. The presence of natural

circulation (with respect to forced circulation) increments the time needed to the SRVs to evacuate the OTSGs secondary side inventory (see different timing collected in Table 7 and trends reported in Figure 10f). The lower primary flow in the steam generator (with respect to the one ensured by forced circulation) decreases the overall heat transfer coefficient and, consequently, the thermal power removed by PCS. This slows down the pressure rise in the secondary system and increases the time interval between two subsequent SRVs openings. With natural circulation, the OTSGs cooling capability lasts more than cases dominated by forced circulation.

Terminated the water inventory in the OTSGs secondary side lower downcomer, the dominant effect on the BZ temperatures is the presence of the decay heat. They start to drift positively. The temperature slope is lower than the one due to forced circulation because of the absence of pumping power. Temperatures rise of 10 °C in the last 4000 s of simulation (nearly 9 °C/hr).

During the cooling transient provided by the steam generators, system pressure decreases unlimited by pressurizer heaters (Figure 10g). They are disabled from the occurrence of turbine trip. Later, once evacuated the OTSGs secondary side inventory (the total mass discharged is provided by Table 7), the system pressure starts to rise. Pressurizer sprays are off since no pumps are available in the circuit. The PORV opening setpoint is reached quite faster (compare timing gathered in Table 7). From this moment, PHTS pressure follows the sawtooth trend already discussed. The trend of water level in the pressurizer (Figure 10h) is similar to the one reported in Figure 8c for LF6 sequence. The parameter evolution and the phenomenology occurring in the component are the same. At the end of the transient, the tank is nearly solid. The total BZ PHTS water mass discharged by PORV at EOT is indicated in Table 7.

4.2.4. LOFA Transients Involving BZ Cooling Circuit

BZ System Transient Evolution

Once PIE occurs, the primary flow elaborated by interested pump/pumps starts to decrease. In LF3 and LF7 transients, only loop 1 MCP 1 is stopped (partial LOFA), while, in LF4 and LF8 sequences, all system pumps are involved in the accident (complete LOFA). Low flow takes few seconds to be detected, actuating the plasma shutdown. Consequently, also turbine trip is triggered. In case LF7, where a loss of off-site power is assumed, TT causes the stop of all the system pumps not interested from initiating event. For this reason, in LF4, LF7 and LF8 scenarios, the coast-down of all the BZ pumps is nearly contemporaneous and these cases have a similar accidental evolution. The only different sequence is LF3, where loop 1 MCP 2 and loop 2 MCPs continue to provide primary coolant flow. They are stopped on high-temperature signal at nearly EOT. Summarizing, for what concerns BZ PHTS, the selected cases can be grouped in the same way already seen for FW PHTS in Section 4.2.3. Main events and parameters related to the transient simulations characterized by PIE involving BZ MCPs are collected in Table 8.

Case LF3

In this case, the loop 1 MCP 2 and the loop 2 MCPs are still active after the turbine trip (off-site power is available). The loop 1 MCP 2 increases the mass flow provided (Figure 11c). The loop 1 branch hosting the failed pump becomes an alternative flow path for the mass flow provided by loop 1 MCP 2. The pressure drops related to this path is less than the ones associated to a BB sector (even with the failed pump acting as a minor head loss). Hence, for loop 1 MCP 2 the curve of the hydraulic resistance decreases and, being a constant rotational velocity imposed as a boundary condition for the component, the result is an increase of the mass flow provided and a drop of the pump head. Instead, the operation of loop 2 pumps is only slightly altered with respect to the nominal state. The transient is dissymmetrical with respect to the toroidal dimension. The sixteen sectors experience different flows (Figure 11a) and, consequently, inlet/outlet COB temperatures (Figure 11b). Higher mass flows (i.e., lower outlet temperatures) correspond to the sectors located in

diametrically opposite position with respect to the failed pump (four of sixteen). However, the forced flow availability significantly smooths the temperature peaks at COB outlet (only few degrees above the nominal value).

Table 8. Summary table for LOFA transients involving BZ PHTS MCPs.

Event/Parameter	Unit	LF3	LF4	LF7	LF8
PIE (LOFA)	-	Partial (BZ)	Complete (BZ)	Partial (BZ)	Complete (BZ)
Loss of off-site power	yes/no	no	no	yes	yes
PT signal occurrence	s	2.5	2.5	2.5	2.5
TT signal occurrence	s	2.5	2.5	2.5	2.5
TSVs start to close	s	2.5	2.5	2.5	2.5
Start of PCS feedwater ramp-down	s	2.5	2.5	2.5	2.5
Start of IHTS mass flow ramp-down	s	10	10	2.5	2.5
Time of FW PHTS water temperature peak	s	-	-	24	23
FW PHTS water temperature peak [1]	°C	-	-	331	331
Time of BZ PHTS water temperature peak	s	30	58	59	59
BZ PHTS water temperature peak [1]	°C	333	340	340	340
FW MCPs Trip occurrence	s	7496	8440	2.5	2.5
BZ MCPs Trip occurrence (pump not interested by PIE)	s	7260	-	2.5	-
Time to evacuate BZ OTSGs secondary side inventory	s	600 (L1) 460 (L2)	2150	2150	2150
Water mass discharged from BZ OTSGs secondary side	kg	15,017 (L1) 17220 (L2)	15,037 (per OTSG)	14,871 (per OTSG)	12,885 (per OTSG)
FW PORV first opening time (Long Term)	s	7332	8576	2248	2284
Total FW PHTS water mass discharged at EOT	kg	1034	247	1444	1356
BZ PORV first opening time (Long Term)	s	6952	4412	4164	4168
Total BZ PHTS water mass discharged at EOT	kg	6113	4592	4541	5025

[1] For all the sixteen sectors, both the BZ and FW PHTS water temperatures were detected at the outlet of COB segment. For each PHTS, peak temperature reported in the table is the maximum among all the temperature readings.

As observed in FW system for case LF1, a flow inversion can be detected in the BZ system branch where the failed pump is located. The pressure drops related to the blanket component are so high that a part of the flow provided by loop 1 MCP 2 is recirculated through this alternative flow path. Differently from LF1 sequence, the reverse flow does not cause a temperature inversion in loop 1. In fact, each loop pump is hosted in a branch going from the OTSG outlet plenum to the cold ring. Even if there is a reverse flow in one of these branches, the primary flow through the hot leg and the steam generator is ensured in the right direction by the operation of the MCP still active. The effect of the failed pump is visible in Figure 11d. The reduced flow in loop 1 with respect to loop 2, slows down the cooling transient provided by the OTSGs in the mid-term. Loop 2 steam generator runs out its cooling capability one hundred seconds earlier than the correspondent in loop 1 (see Table 8 for timing and water mass discharged). From this moment, no sensible differences are detectable between the TH performances of the two loops.

BZ temperatures positively drift since blanket decay heat overwhelms the system heat losses. The temperature slope is of nearly 11 °C/hr (25 °C in 8000 s). This is the same value obtained for BZ system in LF1 and LF2 scenarios, when LOFA transients involve FW PHTS and off-site power is available to ensure the BZ pumps operation. Forced circulation confirms to produce a higher curve slope than the one associated to natural circulation (see Figure 12 related to case LF8). As already discussed, the PHTS coolant additional heating is caused by pumping power. MCPs trip, whose timing is reported in Table 8, is triggered by a high-temperature signal at the pump inlet. Later, forced circulation is lost and natural circulation establishes (Figure 11c). The temperature slope starts to decrease accordingly.

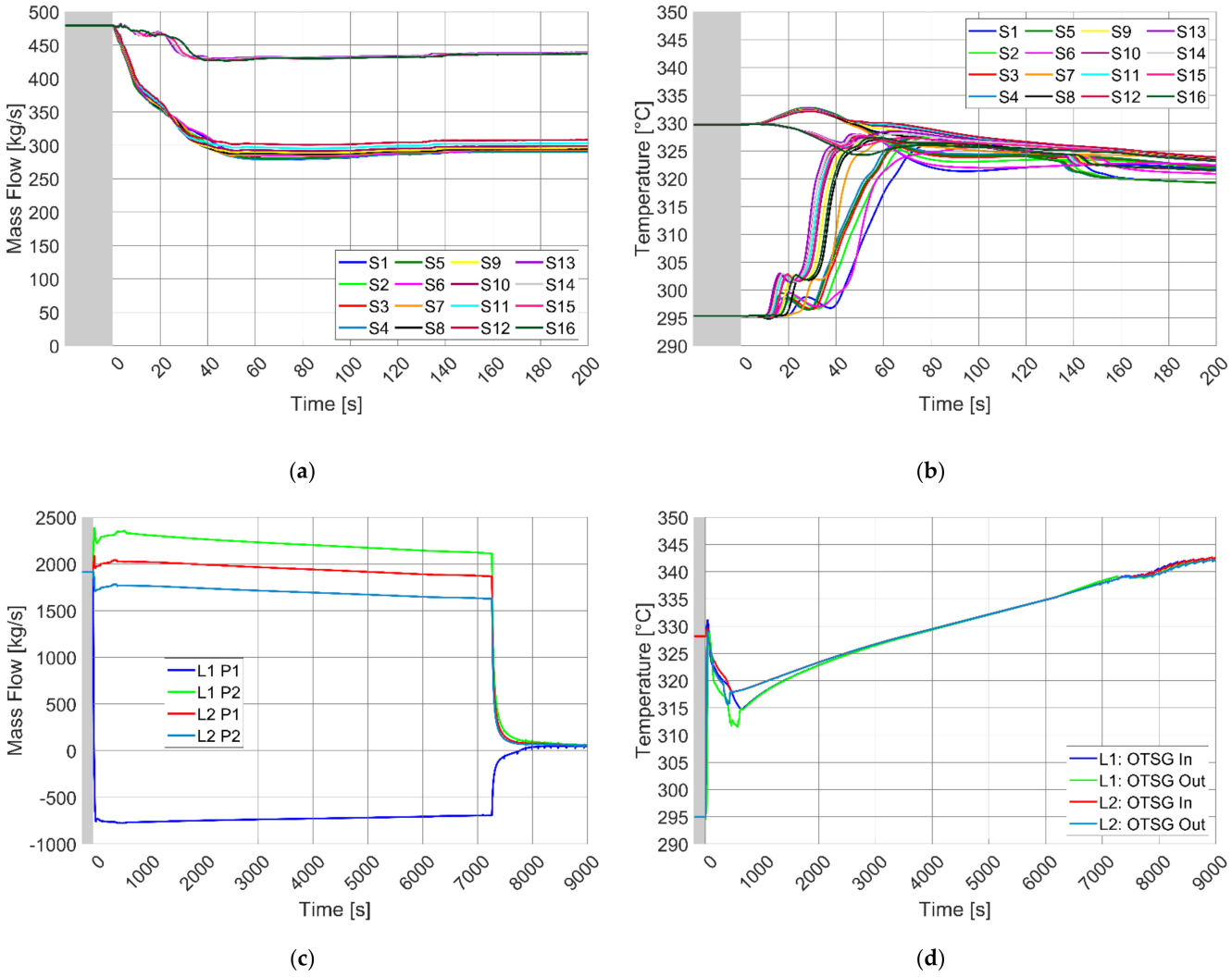

Figure 11. Partial LOFA on BZ PHTS without loss of off-site power (LF3 transient): (**a**) Mass flow in BZ sectors (early time); (**b**) BZ PHTS water temperatures at BB inlet & outlet (all sectors, early time, COB segment); (**c**) Mass flow elaborated by BZ PHTS MCPs (full range); (**d**) BZ PHTS water temperatures at OTSGs inlet & outlet (full range).

The plot of BZ pressure trend is not included in the following since it is the same of LF1 and LF2 transients (see Figure 10g). The presence of pressurizer sprays, ensured by the BZ pumps still active, allows to control the system pressure for nearly two hours. Then, the decay heat is evacuated by discharging PHTS water through the PORV. The relevant parameters are contained in Table 8.

Cases LF4, LF7 and LF8

The considered cases have an accidental evolution very similar to the one described in Section 4.2.3 for LF5 and LF6 sequences. In these scenarios, trip occurs for all the BZ pumps after few seconds from the SOT (see Tables 7 and 8), albeit for different reasons. The resulting transients are quite symmetrical with respect to the toroidal dimension. PHTS temperatures at BB inlet/outlet are the same for all the sectors. They are reported in Figure 12a for LF4, LF7 and LF8 scenarios. Among the different cases, no sensible differences are detectable in the temperature peak at COB outlet. The maximum values, indicated in Table 8, are close to the ones observed for LF5 and LF6 transients (Table 7). Also the BZ system long-term behavior is nearly the same. As an example, the PHTS water temperatures at OTSGs inlet/outlet are plotted for case LF8 in Figure 12b. The trend is very similar to the analogous contained in Figure 10e for LF6 sequence. After

pump coast-down, natural circulation establishes in the system, influencing the BZ thermal-hydraulic performances. A detailed description of the transient evolution is provided in Section 4.2.3, in the paragraph referring to BZ PHTS. A quantitative comparison between all the interested cases can be performed looking at the main timing and TH parameters related to the BZ system contained in Tables 7 and 8.

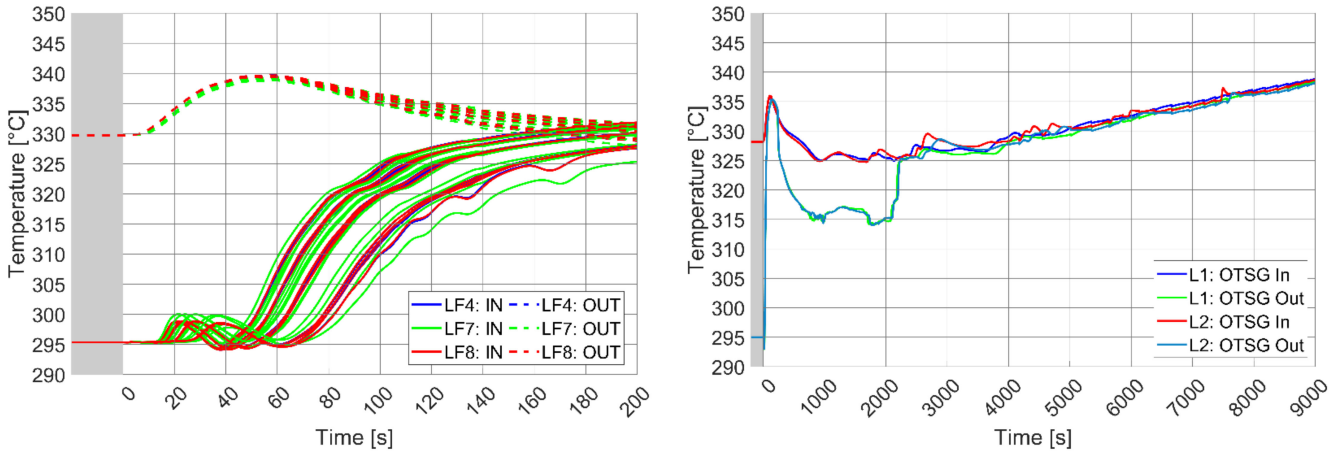

(**a**) (**b**)

Figure 12. Parameter trends in BZ PHTS for LOFA transients characterized by natural circulation (LF4, LF7, LF8): (**a**) BZ PHTS water temperatures at BB inlet & outlet (all sectors, early time, COB segment); (**b**) BZ PHTS water temperatures at OTSGs inlet & outlet (full range, only LF8).

FW System Transient Evolution

Considerations related to FW system are of the same kind of the ones done in Section 4.2.3 about BZ PHTS. FW pumps are not interested from PIE and the system performances are strongly influenced by the presence of off-site power. If available, as in LF3 and LF4 scenarios, FW pumps continue to provide primary flow. The slight parameter decrease is due to the increase of the system average temperature. (Figure 13c). MCPs trip occurs after more than two hours from PIE (Table 8). It is triggered by a high-temperature signal at the pump inlet. The simulation is characterized by the presence of the forced circulation. Instead, if the loss of off-site power is assumed, as in cases LF7 and LF8, FW MCPs trip occurs following the turbine trip and forced circulation is lost few seconds after SOT (Figure 13c). Natural circulation establishes in the FW system, influencing its TH behavior during the overall simulation.

Forced Circulation (LF3 and LF4 Cases)

Due to the presence of forced circulation, FW temperatures converge very quickly to an average value (Figure 13d). Transient is symmetrical with respect to toroidal dimension and, for all the BB sectors, no temperature peak is present at blanket outlet (Figure 13a). HITEC® secondary flow is available for the first 10 s after PIE. This element, combined with the suitability of forced circulation in the primary system, avoids the opening of the pressurizer PORV in the early time (Figure 13b).

In the long term, FW HEXs are not able to provide any cooling capability and system heat losses do not counterbalance the blanket decay heat. An additional source term is represented by the pumping power. FW temperatures start to drift positively (Figure 13d). The associated temperature slope is of nearly 11 °C/hr (20 °C in 7000 s). The Eurofer maximum temperature in the FW component follows the same time trend of the PHTS water (Figure 13e). Once MCPs trip is triggered, the forced circulation is lost and the

natural circulation establishes. The temperature slope decreases to the value related to simulations characterized by natural circulation (LF7 and LF8 scenarios).

Pressure transient for the considered cases (Figure 13f) is similar to the one described for LF1 sequence (see Section 4.2.3 and Figure 8b). After the heat sink loss, FW pressure is limited by pressurizer sprays. When sprays become unable to perform their control function (due to system temperature increase), the management of system pressure switches to PORV component (timing of this event is reported in Table 8). The total mass discharged from the valve at EOT is indicated in Table 8. The plot of pressurizer level related to cases LF3 and LF4 is not included in the following since very similar to the one reported in Figure 8c for LF1 transient.

Natural Circulation (LF7 and LF8 Cases)

For the considered cases, plasma shutdown, turbine trip, FW MCPs trip and IHTS mass flow ramp-down occur at the same time. The PHTS water temperatures at COB inlet/outlet are collected, for all the sectors, in Figure 13a. Their trends result from the relative balance between plasma power, primary flow and secondary flow, all decreasing parameters but with different timing. COB outlet temperatures experience a slight increase since initially the plasma power is prevalent. Then, since the pump coast-down (Figure 13c) takes more time than the plasma shutdown (Table 6) the outlet temperatures start to decrease. Peak value is the same for all the sectors and for all the cases, as reported in Table 8.

Due to the unavailability of forced circulation in both primary and secondary systems, the initial power surplus produces a sudden increase in the FW PHTS pressure, Figure 13b. Pressurizer PORV intervenes to manage this pressure transient.

During the FW pump coast-down, system reaches a quite uniform temperature (Figure 13d). Later, while natural circulation establishes, system temperatures experience an inversion. In the long term, the original temperature field is restored and FW temperatures positively drift. The temperature slope is lower (nearly 9 °C/hr) than the one observed for cases LF3 and LF4, since the additional source term due to pumping power is missing.

After FW MCPs trip, pressurizer sprays are disabled. System Pressure increase can be only limited by the PORV intervention (Figure 13f). The valve opening occurs quite earlier with respect to LF3 and LF4 sequences (compare different timing reported in Table 8). From this moment, the system pressure begins to cycle accordingly with the valve component multiple interventions. The PHTS mass discharged at the EOT is indicated in Table 8.

Figure 13e reports the trend of the maximum Eurofer temperature in the FW component. The peak related to PHTS water present at blanket outlet (Figure 13a) here is not visible. Temperature excursion is smoothed by the FW thermal inertia, even if low. After plasma termination, material temperature drops driven by PHTS water temperature. Instead, in the long term, FW component is heated up by the decay heat. The temperature slope is the same of the PHTS water trend.

Summarizing, the considered cases have accidental evolutions very similar to the one described in Section 4.2.3 for LF2, LF5 and LF6 transients. The common factor to all these scenarios is the occurrence of FW MCPs trip after few seconds from the SOT (see Tables 7 and 8), albeit for different reasons. Hence, the forced circulation is immediately lost and the natural circulation influences the system TH performances during the overall simulation. A qualitative comparison between the interested cases can be performed by looking at the parameter trends collected in Figures 8 and 9 (where LF6 sequence was used as reference) and Figure 13 (using LF8 as selected scenario). For the same purpose, but from a quantitative point of view, parameters and timing contained in Tables 7 and 8 can be used.

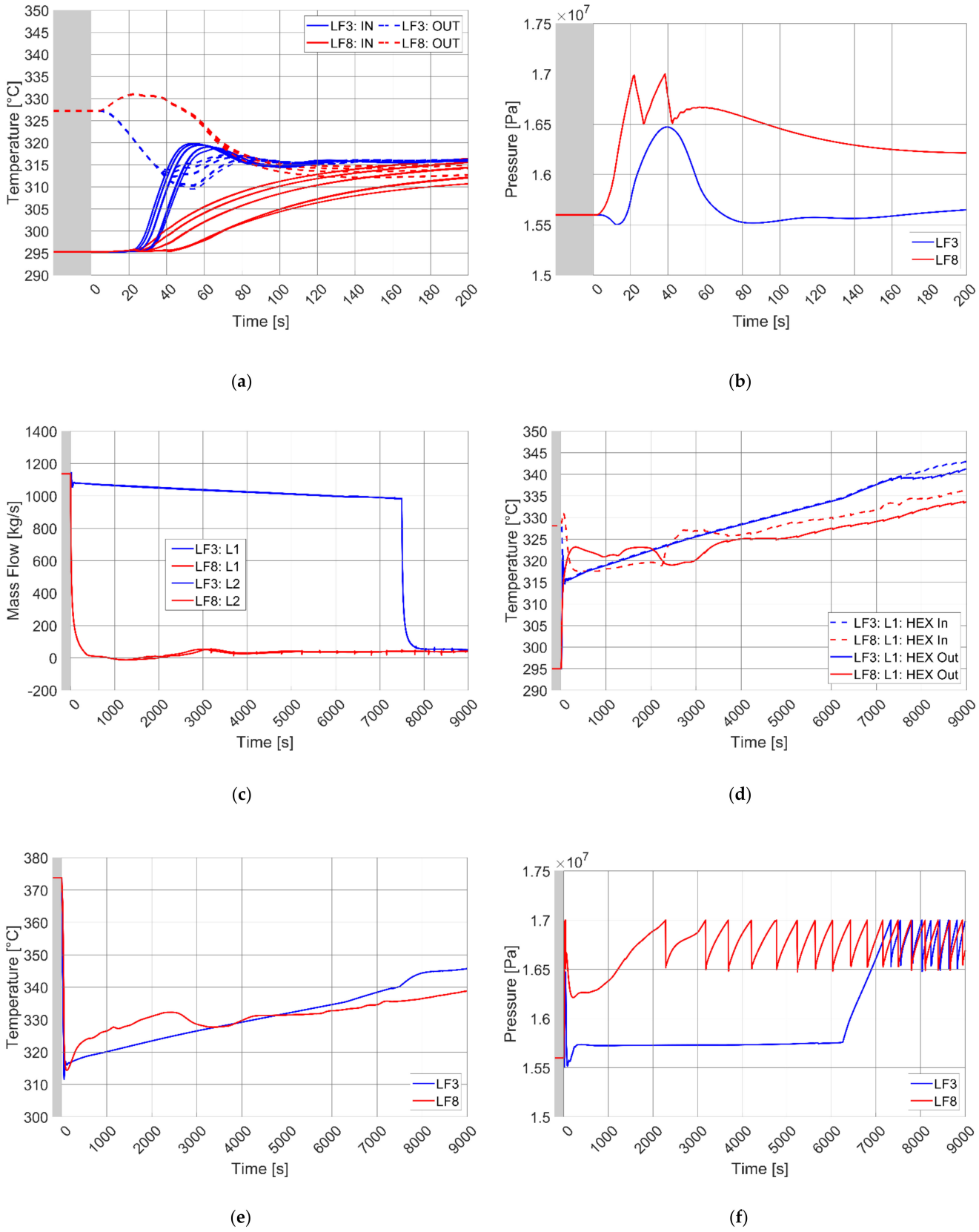

Figure 13. Comparison between LF3 and LF8 transients: (**a**) FW PHTS water temperatures at BB inlet & outlet (all sectors, early time, COB segment); (**b**) Pressure in FW PHTS (early time); (**c**) Mass flow elaborated by FW MCPs (full range); (**d**) FW PHTS water temperatures at HEX inlet & outlet (loop 1, full range); (**e**) Maximum Eurofer temperature in FW component (full range); (**f**) Pressure in FW PHTS (full range).

5. Discussion

Results presented in the previous section highlight how the type of circulation (natural or forced) characterizing each cooling system is the main element influencing its TH performances. According to the considered case, BZ and FW systems can have the same kind of circulation or not. However, as a general rule, for the suitability of the forced circulation in a primary cooling circuit is mandatory the presence of the off-site power. If its loss is assumed in combination with the initiating event, at the occurrence of turbine trip forced circulation is lost in both systems, if not already missing in one of them according to the specific PIE considered. In fact, the turbine generator set is the only element ensuring the AC power needed for the pumps operation and it is disconnected after the TT signal. If forced circulation is available, the following TH behavior can be observed in BZ and FW systems.

- Few seconds after the SOT, the temperature spikes at blanket outlet characterizing the trend of both BZ and FW PHTS water are significantly smoothed.
- In FW system, the availability of forced circulation in both primary and secondary (only for the first 10 s) circuits limits the pressure increase and avoids the intervention of the pressurizer PORV in the short term.
- The OTSGs cooling capability lasts less. The presence of forced circulation in the primary cooling system enhances the steam generator HTC, increasing the thermal power transferred to the PCS. This reduces the time between two subsequent steam line SRVs openings and speeds up the evacuation of the water mass present in the OTSGs secondary side. Once terminated, the steam generators are no more able to provide any cooling function to the BZ PHTS.
- For more or less two hours from PIE occurrence, the system pressure is controlled by the pressurizer sprays. The first PORV intervention in the long term is significantly delayed.
- The temperature slope characterizing both BZ and FW systems (thermally coupled) is higher since pumping power is added to the power balance. This is valid until the MCPs trip is triggered in each system.

Summarizing, forced circulation improves the BZ and FW TH performances in the short term, smoothing the temperature spikes, but reduces the ones in the mid-long term. In fact, it shortens the cooling interval provided to the BZ PHTS by the steam generators and increases the temperature slope experienced by BZ and FW systems, reducing the reactor grace time. The best management strategy for PHTS pumps is to use, at the SOT, the forced circulation they provide, in order to avoid excessive temperatures in the blanket, and then stop them, to increase the reactor grace time. To prove the effectiveness of this control logic, case LF3 was run again adding a new trip signal to BB MCPs. The level in the BZ OTSGs lower downcomer is monitored and when it reaches the 1% of the rated value in full plasma power state, both BZ and FW pumps are stopped. LF3 (partial LOFA in BZ PHTS without loss of off-site power) was selected as reference case since it is one of the two (together with LF1) where forced circulation is available for both primary cooling systems, even if reduced in the one involved in the PIE. The PHTS water temperatures at loop 1 OTSG/HEX inlet/outlet are reported in Figure 14. As shown, this new pump management strategy combines the benefits of forced circulation in the short term and of natural circulation in the long term.

In all the transient simulations, included the one discussed in this section, BZ and FW systems experience a positive temperature drift in the mid-long term. It is due to the unbalance between decay heat produced in the blanket and system heat losses, with the former overwhelming the latter. The temperature slope is higher if the forced circulation is still active. In these cases, it must be added another source term to the power balance, represented by the pumping power. In the calculations performed, no Decay Heat Removal (DHR) system was implemented in the input deck and the power surplus is managed by the pressurizer PORV. Power in excess produces a pressure increase and when this parameter reaches the PORV opening setpoint, PHTS water mass is discharged with its

associated enthalpy content. This is the way adopted by BZ and FW system to dissipate the power surplus. However, a DHR system is foreseen for DEMO reactor in accidental conditions, as discussed in [5].

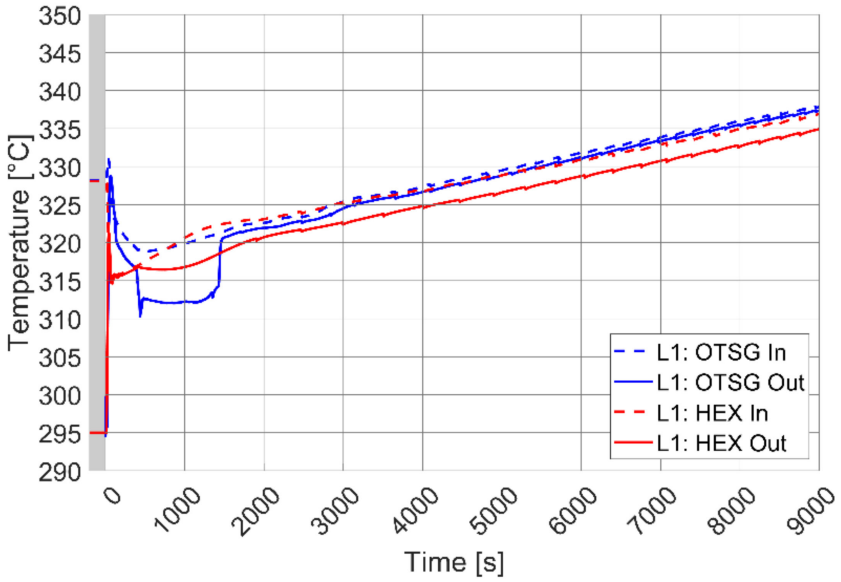

Figure 14. Partial LOFA on BZ PHTS without loss of off-site power, new BB MCPs management strategy: BZ PHTS water temperatures at loop 1 OTSG inlet & outlet and FW PHTS water temperatures at loop 1 HEX inlet & outlet (full range).

6. Conclusions

The analysis was performed with the aim of preliminary evaluating the WCLL BB PHTS behavior during anticipated transients and accidental conditions. A best-estimate system code, RELAP5/Mod3.3, was used to achieve this goal. A modified version was developed at DIAEE with the purpose of increasing the predictive capabilities of the code with respect to fusion reactors. Implemented features include new HTC correlations, new fluids, etc. A full RELAP5 TH model was prepared. Blanket was simulated with equivalent pipes, maintaining the overall thermal inertia. The PHTS cooling circuits were modelled in detail adopting one-dimensional hydrodynamic components. All the system equipment (pumps, heat exchangers, pressurizer) and piping were included in the model. The input deck was initially used to simulate the DEMO full plasma power state, that is the most challenging scenario during the reactor normal operations. This state was chosen as initial condition for the transient analysis. The selected initiating events consist in partial and complete LOFA. Simulations were run considering the PIEs occurring in both BZ or FW system and they were repeated also assuming the loss of off-site power. A matrix of interesting scenarios was individuated. A preliminary actuation logic, based on the consolidated PWR experience and the innovations related to GEN III+ nuclear reactor design, was proposed and implemented for some reactor components. Simulation outcomes highlight the appropriateness of the current PHTS design. BB temperatures do not experience excessive excursions during the plasma shutdown. Pressure transients in BZ PHTS, FW PHTS and PCS are effectively managed by the related relief systems. The results underline a strong dependence of the PHTS TH performances on the type of circulation characterizing each primary cooling circuit. The forced circulation is of great importance in the management of the initial power transient, while the natural circulation is advisable in the long term to increase the reactor grace time. On the basis of the calculation outcomes, a revised BB MCPs management strategy was defined for the cases where the off-site power is available. It combines the short term benefits of forced circulation and the long term advantages of natural circulation. In the long term, BZ and FW systems are heated up

by the BB decay heat, overwhelming the system heat losses. In the current simulations, the power surplus is dissipated by the pressurizer PORV that opens and discharges PHTS water mass and related enthalpy. In the future developments of the activity, the DHR system foreseen for DEMO reactor will be implemented in the input deck to evaluate the effectiveness of its mitigation action.

Author Contributions: Conceptualization, C.C., F.G., A.D.N. and G.C.; methodology, C.C. and F.G.; software, C.C.; validation, C.C. and F.G.; formal analysis, C.C.; writing—original draft preparation, C.C.; writing—review and editing, F.G., A.D.N. and G.C.; supervision, F.G., A.D.N. and G.C.; project administration, A.D.N. and G.C. All authors have read and agreed to the published version of the manuscript.

Funding: This research was funded by Euratom research and training programme 2014-2018 and 2019-2020, grant number 633053.

Institutional Review Board Statement: Not applicable.

Informed Consent Statement: Not applicable.

Data Availability Statement: No new data were created or analyzed in this study. Data sharing is not applicable to this article.

Acknowledgments: This work has been carried out within the framework of the EUROfusion Consortium and has received funding from the Euratom research and training programme 2014–2018 and 2019–2020 under grant agreement No 633053. The views and opinions expressed herein do not necessarily reflect those of the European Commission.

Conflicts of Interest: The authors declare no conflict of interest.

Abbreviations

AC	Alternating Current
BB	Breeding Blanket
BC	Boundary Condition
BRC	Breeding Cell
BOL	Beginning Of Life
BZ	Breeder Zone
CAD	Computer Aided Design
CFETR	China Fusion Engineering Test Reactor
COB	Central Outboard Blanket
CV	Control Volume
DHR	Decay Heat Removal System
DIAEE	Dipartimento di Ingegneria Astronautica, Elettrica ed Energetica
DWT	Double Walled Tube
EOL	End Of Life
EOT	End Of Transient
ESS	Energy Storage System
EU-DEMO	European Demonstration Power Plant
FP	Feeding Pipe
FW	First Wall
HCPB	Helium Cooled Pebble Bed
HCSG	Helicoidal Coil Steam Generator
HEX	Heat EXchanger
HS	Heat Structure
HTC	Heat Transfer Coefficient
IB	Inboard Blanket
IHTS	Intermediate Heat Transfer System
K-DEMO	Korean Demonstration Power Plant
LIB	Left Inboard Blanket
LiPb	Lithium Lead
LOB	Left Outboard Blanket

LOCA	Loss of coolant accident
LOFA	Loss of flow accident
LOHS	Loss of Heat Sink
MARS-KS	Multi-dimensional Analysis of Reactor Safety
MCP	Main Coolant Pump
MS	Molten Salt
OB	Outboard Blanket
OTSG	Once-Through Steam Generator
PCS	Power Conversion System
PHTS	Primary Heat Transfer System
PIE	Postulated Initiating Event
PORV	Pilot (Power)-Operated Relief Valve
PRZ	Pressurizer
PT	Plasma Termination
PWR	Pressurized Water Reactor
RELAP5	Reactor Excursion Leak Analysis Program
RIB	Right Inboard Blanket
ROB	Right Outboard Blanket
SMS	Single Module Segment
SOT	Start Of Transient
SRV	Safety Relief Valve
TH	Thermal-Hydraulics
TSV	Turbine Stop Valve
TT	Turbine Trip
WCCB	Water-Cooled Ceramic Breeder
WCLL	Water-Cooled Lithium-Lead

References

1. Federici, G.; Boccaccini, L.; Cismondi, F.; Gasparotto, M.; Poitevin, Y.; Ricapito, I. An overview of the EU breeding blanket design strategy as an integral part of the DEMO design effort. *Fusion Eng. Des.* **2019**, *141*, 30–42. [CrossRef]
2. Del Nevo, A.; Arena, P.; Caruso, G.; Chiovaro, P.; Di Maio, P.A.; Eboli, M.; Edemetti, F.; Forgione, N.; Forte, R.; Froio, A.; et al. Recent progress in developing a feasible and integrated conceptual design of the WCLL BB in EUROfusion project. *Fusion Eng. Des.* **2019**, *146*, 1805–1809. [CrossRef]
3. Ricapito, I.; Cismondi, F.; Federici, G.; Poitevin, Y.; Zmitko, M. European TBM programme: First elements of RoX and technical performance assessment for DEMO breeding blankets. *Fusion Eng. Des.* **2020**, *156*, 111584. [CrossRef]
4. Martelli, E.; Giannetti, F.; Caruso, G.; Tarallo, A.; Polidori, M.; Barucca, L.; Del Nevo, A. A Study of EU DEMO WCLL breeding blanket and primary heat transfer system integration. *Fusion Eng. Des.* **2018**, *136*, 828–833. [CrossRef]
5. Barucca, L.; Bubelis, E.; Ciattaglia, S.; D'Alessandro, A.; Del Nevo, A.; Giannetti, F.; Hering, W.; Lorusso, P.; Martelli, E.; Moscato, I.; et al. Pre-conceptual design of EU DEMO balance of plant systems: Objectives and challenges. *Fusion Eng. Des.* **2017**. under review.
6. Martelli, E.; Giannetti, F.; Ciurluini, C.; Caruso, G.; Del Nevo, A. Thermal-hydraulic modeling and analyses of the water-cooled EU DEMO using RELAP5 system code. *Fusion Eng. Des.* **2019**, *146*, 1121–1125. [CrossRef]
7. Idaho National Laboratory; The RELAP5-3D© Code Development Team. *RELAP5-3D© Code Manual: Code Structure, System Models, and Solution Methods*; Revision 4.3, INL-MIS-15-36723; Idaho National Laboratory: Idaho Falls, ID, USA, 2015; Volume I.
8. Emonot, P.; Souyri, A.; Gandrille, J.L.; Barré, F. CATHARE-3: A new system code for thermal-hydraulics in the context of the NEPTUNE project. *Nucl. Eng. Des.* **2011**, *241*, 4476–4481. [CrossRef]
9. Hu, R. A fully-implicit high-order system thermal-hydraulics model for advanced non-LWR safety analyses. *Ann. Nucl. Energy* **2017**, *101*, 174–181. [CrossRef]
10. D'Onorio, M.; Giannetti, F.; Porfiri, M.T.; Caruso, G. Preliminary safety analysis of an in-vessel LOCA for the EU-DEMO WCLL blanket concept. *Fusion Eng. Des.* **2020**, *155*, 111560. [CrossRef]
11. D'Onorio, M.; Giannetti, F.; Porfiri, M.T.; Caruso, G. Preliminary sensitivity analysis for an ex-vessel LOCA without plasma shutdown for the EU DEMO WCLL blanket concept. *Fusion Eng. Des.* **2020**, *158*, 111745. [CrossRef]
12. Gauntt, R.O.; Cash, J.E.; Cole, R.K.; Erickson, C.M.; Humphries, L.L.; Rodriguez, S.B.; Young, M.F. *MELCOR Computer Code Manuals: Primer and Users*; Guide Version 1.8.6., Revision 3, NUREG/CR-6119; Sandia National Laboratory: Albuquerque, NM, USA, 2005; Volume 1.
13. D'Onorio, M.; Caruso, G. Pressure suppression system influence on vacuum vessel thermal-hydraulics and on source term mobilization during a multiple First Wall-Blanket pipe break. *Fusion Eng. Des.* **2021**, *164*, 112224. [CrossRef]

14. Ciurluini, C.; Giannetti, F.; Martelli, E.; Del Nevo, A.; Barucca, L.; Caruso, G. Analysis of the thermal-hydraulic behavior of the EU-DEMO WCLL Breeding Blanket cooling systems during a Loss Of Flow Accident. *Fusion Eng. Des.* **2021**, *164*, 112206. [CrossRef]
15. The US Nuclear Regulatory Commission (USNRC). *RELAP5/MOD3 Code Manual: Code Structure, System Models, and Solution Methods*; NUREG/CR-5535; USNRC: Washington, DC, USA, 1998; Volume I.
16. D'Amico, S.; Di Maio, P.A.; Jin, X.Z.; Hernández-Gonzalez, F.A.; Moscato, I.; Zhou, G. Preliminary thermal-hydraulic analysis of the EU-DEMO Helium-Cooled Pebble Bed fusion reactor by using the RELAP5-3D system code. *Fusion Eng. Des.* **2021**, *162*, 112111. [CrossRef]
17. Jin, X.Z.; Chen, Y.; Ghidersa, B.E. LOFA analysis for the FW of DEMO HCPB blanket concept. In Proceedings of the 1st IAEA Technical Meeting on the Safety, Design and Technology of Fusion Power Plants, Vienna, Austria, 3–5 May 2016.
18. Jin, X.Z. BB LOCA analysis for the reference design of the EU DEMO HCPB blanket concept. *Fusion Eng. Des.* **2018**, *136 Pt B*, 958–963. [CrossRef]
19. Cheng, X.; Ma, X.; Li, X.; Wang, W.; Liu, S. Steady states and LOFA analyses of the updated WCCB blanket for multiple fusion power modes of CFETR. *Fusion Eng. Des.* **2019**, *144*, 23–28. [CrossRef]
20. Cheng, X.; Lin, S.; Liu, S. Loss of flow accident and loss of heat sink accident analyses of the WCCB primary heat transfer system for CFETR. *Fusion Eng. Des.* **2019**, *147*, 111247. [CrossRef]
21. Moon, S.B.; Lim, S.M.; Bang, I.C. Analysis of hydrogen and dust explosion after vacuum vessel rupture: Preliminary safety analysis of Korean fusion demonstration reactor using MELCOR. *Int. J. Energy Res.* **2018**, *42*, 104–116. [CrossRef]
22. Cheng, X.; Ma, X.; Lu, P.; Wang, W.; Liu, S. Thermal dynamic analyses of the primary heat transfer system for the WCCB blanket of CFETR. *Fusion Eng. Des.* **2020**, *161*, 112067. [CrossRef]
23. Kim, G.-W.; Lee, J.-H.; Cho, H.-K.; Park, G.-C.; Im, K. Development of thermal-hydraulic analysis methodology for multiple modules of water-cooled breeder blanket in fusion DEMO reactor. *Fusion Eng. Des.* **2016**, *103*, 98–109. [CrossRef]
24. Jeong, J.-J.; Ha, K.S.; Chung, B.D.; Lee, W.J. Development of a multi-dimensional thermal-hydraulic system code, MARS 1.3.1. *Ann. Nucl. Energy* **1999**, *26*, 1611–1642. [CrossRef]
25. Giannetti, F.; D'Alessandro, T.; Ciurluini, C. *Development of a RELAP5 Mod3.3 Version for FUSION Applications*; DIAEE Sapienza Technical Report No. D1902_ENBR_T01, Revision 1; DIAEE, Sapienza University of Rome: Rome, Italy, 2019.
26. Edemetti, F.; Micheli, P.; Del Nevo, A.; Caruso, G. Optimization of the first wall cooling system for the DEMO WCLL blanket. *Fusion Eng. Des.* **2020**, *161*, 111903. [CrossRef]
27. Edemetti, F.; Di Piazza, I.; Del Nevo, A.; Caruso, G. Thermal-hydraulic analysis of the DEMO WCLL elementary cell: BZ tubes layout optimization. *Fusion Eng. Des.* **2020**, *160*, 111956. [CrossRef]
28. Idelchik, I.E. *Handbook of Hydraulic Resistance*, 2nd ed.; Hemisphere Publishing Corporation: Washington, DC, USA, 1986.
29. Sieder, E.N.; Tate, G.E. Heat transfer and pressure drop of liquids in tubes. *J. Ind. Eng. Chem.* **1936**, *28*, 1429–1435. [CrossRef]
30. U.S. Nuclear Regulatory Commission. Section 3.2—Reactor Coolant System. In Westinghouse Technology Systems Manual. 2012. Available online: https://www.nrc.gov/docs/ML1122/ML11223A213 (accessed on 10 March 2021).
31. U.S. Nuclear Regulatory Commission. Section 10.2—Pressurizer Pressure Control System. In Westinghouse Technology Systems Manual. 2012. Available online: https://www.nrc.gov/docs/ML1122/ML11223A287 (accessed on 10 March 2021).
32. Spagnuolo, A. *BB-9.2.1-T010-D005: Breeding Blanket Load Specifications Document*; EUROfusion Internal Deliverable, EFDA_D_2NLL6N v1.1; EUROfusion: Garching, Germany, 2019.